2.8. Immunohistochemical study

Paraffin-embedded heart sections were washed in increasing concentrations of ethanol and then with PBS. Sections were incubated with Protein Block (DakoCytomation, Glostrup, Denmark), then with mouse anti-rat von Willebrand Factor (vWF) (DakoCytomation), CD68 (DakoCytomation) or monocyte chemoattractant protein-1 (MCP-1) (BD Biosciences Pharmingen, San Jose, CA, USA) antibody in diluent for 40 min, followed by incubation with horseradish peroxidase (HRP)-linked rabbit anti-mouse IgG (DakoCytomation) for 30 min. Sections were visualized using 0.5% diaminobenzidine and 0.03% hydrogen peroxide, and counterstained with hematoxylin. The numbers of CD68-stained cells and vWF-stained capillaries were determined in 10 randomly selected fields (×200).

2.9. Enzyme-linked immunosorbent assay (ELISA)

Serum MCP-1 level of rats on day 21 post-myosin injection was measured using a Rat MCP-1 ELISA kit (Biosource International, Carmarillo, CA, USA). Vascular endothelial growth factor (VEGF) and hepatocyte growth factor (HGF) levels in the supernatant of MSC culture (2.3×10^5 cells in 10-cm dish cultured for 48 h) were measured using ELISA kits, according to the manufacturers' protocols (HGF, Institute of Immunology, Tokyo, Japan; VEGF, R&D Systems, Minneapolis, MN, USA).

2.10. Isolation of cardiomyocytes

Ventricular cardiomyocytes were obtained as described previously with modification [9]. Briefly, after heparinization by intraperitoneal injection of 1000 U/kg heparin sodium, the heart was rapidly excised, and pulmonary, connective and other noncardiac tissues were removed. The heart was then mounted on the cannula of a modified Langendorff apparatus and perfused with buffer containing 0.75 mg/ml collagenase type I (Worthington, Lakewood, NJ, USA), 0.5 mg/ml hyaluronidase (Sigma) and 1% bovine serum albumin (fraction V, ICN, Aurora, OH, USA), in a recirculating fashion for 3 h. After the perfusion sequence, the heart was removed from the perfusion apparatus, the atrium was removed, and gently minced. The enzyme-containing buffer was harvested and the cardiomyocytes resuspended in fresh buffer. The calcium concentration in the suspension was raised stepwise to 1.2 mM. Quiescent, calcium-tolerant cardiomyocytes were gravitationally separated from any nonventricular cells and resuspended in complete culture medium. The culture medium was exchanged for fresh medium to remove the damaged myocytes that failed to attach 3 h after plating. After this procedure, 80% to 90% myocytes were viable and showed rod-shape.

2.11. Cardiomyocyte stimulation and MTS assay

To assess cardioprotective effects of MSC acting in a paracrine manner, we investigated whether conditioned medium obtained from MSC culture attenuated MCP-1-induced cardiomyocyte injury. Cardiomyocytes were plated on 96-well plates (1×10^3 viable cells/well) precoated with laminin (BD Biosciences Pharmingen). After 3 h, the medium was changed to fresh DMEM containing 15% FBS or conditioned medium obtained from MSC culture, with or without 50 ng/ml MCP-1 (R&D Systems, Minneapolis, MN, USA). After 24 h, the cellular level of 3-(4,5-dimethylthiazol-2-yl)-5-(3-carboxymethoxyphenyl)-2-(4-sulfophenyl)-2H-tetrazolium (MTS), indicative of the mitochondrial function in living cells and cell viability, was measured ($n=6$) with a CellTiter96 AQueous One Kit (Promega, Madison, WI, USA) and a Microplate Reader (490 nm, Bio-Rad, Hercules, CA, USA).

2.12. In vitro apoptosis assay

Terminal dUTP nick end labeling (TUNEL) assay (ApopTag Fluorescein In Situ Apoptosis Detection Kit, Chemicon International, Temecula, CA, USA) was performed to evaluate apoptosis of cultured cardiomyocytes. After incubation for 24 h, cardiomyocytes were fixed in 1% paraformaldehyde, and TUNEL staining was performed for detection of apoptotic nuclei according to the manufacturer's

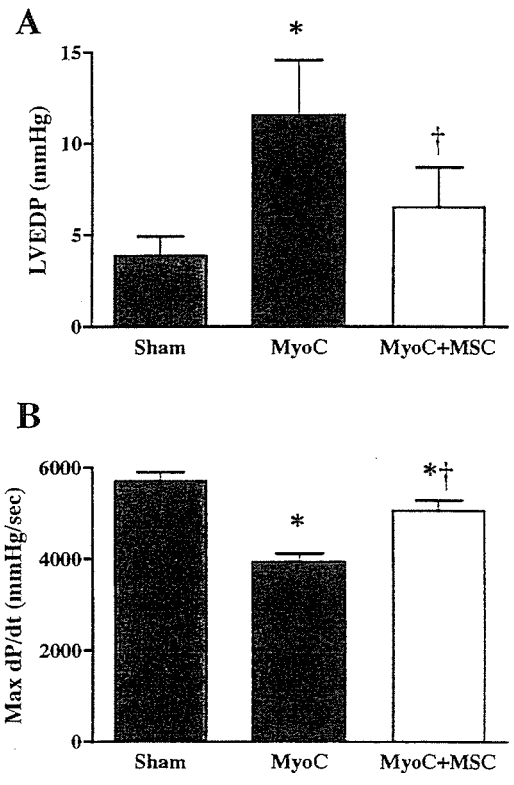

Fig. 1. Effects of MSC transplantation on hemodynamic parameters in acute myocarditis. (A) Left ventricular end-diastolic pressure (LVEDP) and (B) maximum dP/dt (Max dP/dt) were measured in sham-operated rats given vehicle (Sham group), myosin-treated rats given vehicle (MyoC group), and myosin-treated rats given MSC (MyoC+MSC group). Values are mean±S.E. *$P<0.05$ *vs* Sham, †$P<0.05$ *vs* MyoC group.

Table 1
Physiological parameters in three experimental groups

	Sham	MyoC	MyoC+MSC
HW/BW (g/kg)	2.9±0.3	6.4±0.3*	4.7±0.3*,†
HR (bpm)	446±11	363±14*	442±12*,†
MAP (mm Hg)	108±3	87±3*	108±4†
LVSP (mm Hg)	130±2	105±4*	125±4†
Min d*P*/d*t* (mm Hg/s)	−5440±199	−3097±183*	−4617±171*,†

Sham, sham-operated rats given vehicle; MyoC, myosin-treated rats given vehicle; MyoC+MSC, myosin-treated rats given MSC (3×10^6 cells); HW/BW, heart weight to body weight ratio; HR, heart rate; MAP, mean arterial pressure; LVSP, left ventricular systolic pressure; Mim d*P*/d*t*, minimum d*P*/d*t*. Data are mean±S.E. *$P<0.05$ *vs* Sham, †$P<0.05$ *vs* MyoC group.

instructions. The cells were then mounted in medium containing DAPI. Randomly selected microscopic fields ($n=5$) were evaluated to calculate the ratio of TUNEL-positive cells to total cells.

Table 2
Echocardiographic findings in three experimental groups

	Sham	MyoC	MyoC+MSC
LVDs (mm)	3.1±0.1	5.0±0.4*	3.8±0.2†
EF (%)	74.9±1.2	56.6±3.4*	71.2±3.5†
AWT diastole (mm)	1.9±0.1	3.0±0.2*	3.0±0.3*
PWT diastole (mm)	1.9±0.1	3.4±0.1*	2.7±0.2*,†

Sham, sham-operated rats given vehicle; MyoC, myosin-treated rats given vehicle; MyoC+MSC, myosin-treated rats given MSC (3×10^6 cells); LVDs, left ventricular systolic dimension; EF, ejection fraction; AWT, anterior wall thickness; PWT, posterior wall thickness. Data are mean±S.E. *$P<0.05$ *vs* Sham, †$P<0.05$ *vs* MyoC group.

2.13. Creatine kinase (CK) activity assay

CK activity in culture media was measured after incubation of cardiomyocytes for 24 h ($n=5$), using the enzyme measurement kit (Kanto Chemical, Tokyo, Japan).

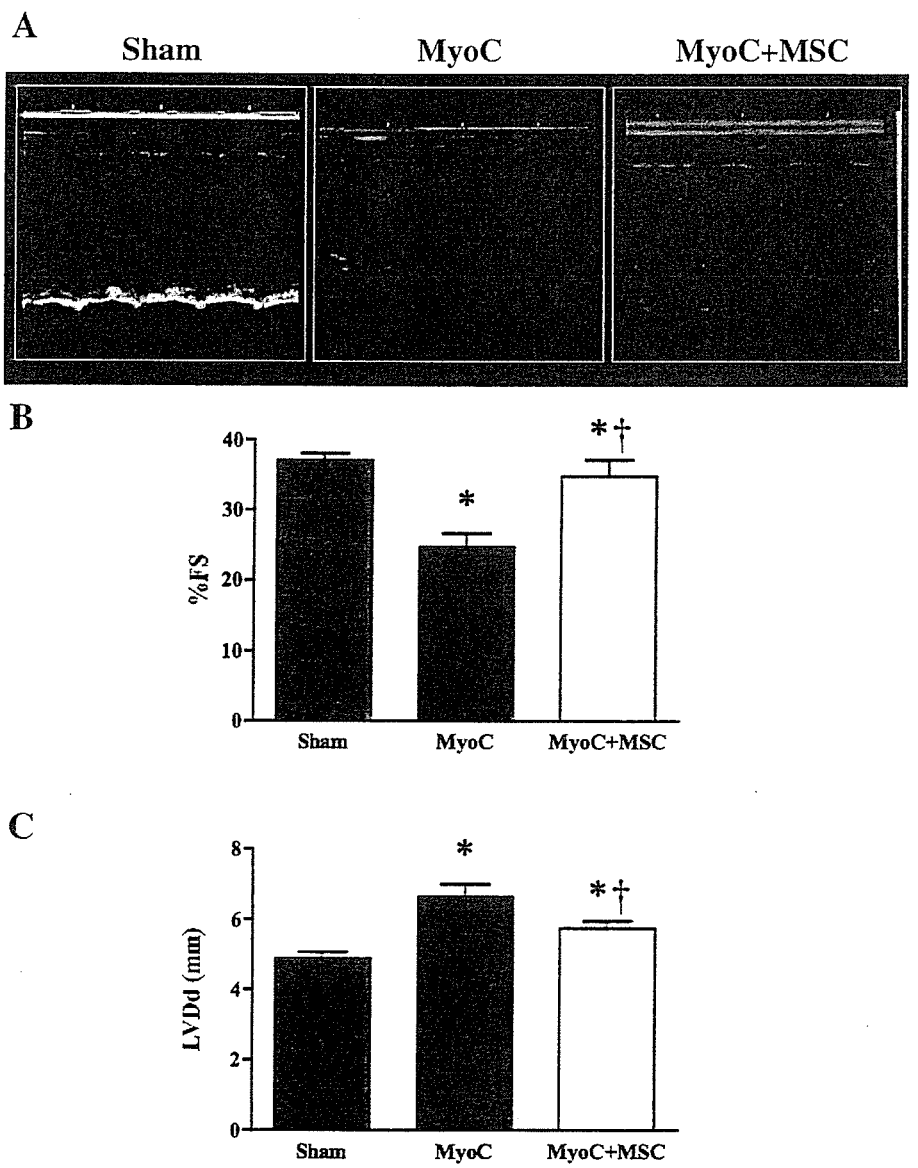

Fig. 2. Effects of MSC transplantation on echocardiographic parameters in acute myocarditis. (A) Representative echocardiographic images showing wall thickening and poor movement in the MyoC group, and improvement of cardiac contractility in the MyoC+MSC group. (B and C) MSC transplantation significantly improved fractional shortening (%FS) and left ventricular diastolic dimension (LVDd). Values are mean±S.E. *$P<0.05$ *vs* Sham, †$P<0.05$ *vs* MyoC group.

2.14. Statistical analysis

Data were expressed as mean ± standard error (S.E.). Comparisons of parameters among groups were made by one-way ANOVA, followed by Newman–Keuls' test. Differences were considered significant at $P<0.05$.

3. Results

3.1. Improvement in cardiac function by MSC transplantation

Two of 15 rats in the MyoC group died on day 19 and day 21 post-myosin injection, respectively, whereas the MyoC+MSC group had no mortality. At 3 weeks post-myosin injection, the MyoC group showed increased heart weight/body weight ratio (HW/BW) and LVEDP, and decreased MAP and Max d*P*/d*t* compared with the Sham group, indicating the presence of acute heart failure in this model (Fig. 1 and Table 1). These parameters subsequently returned to baseline with MSC transplantation (MyoC+MSC group). On echocardiography, the MyoC group showed an increase in LVDs and LVDd, and a significant reduction in %FS and EF (Fig. 2 and Table 2). MSC transplantation significantly improved these parameters (MyoC+MSC group).

3.2. Attenuation of myocardial inflammation by MSC transplantation

Myocardial necrosis and tissue granulation as well as giant cell infiltration and edema were markedly increased in our model of acute myocarditis (Fig. 3A). MSC transplantation significantly attenuated these changes observed in the MyoC group. MSC-transplanted hearts exhibited a consistent tendency for a reduction of tissue granulation, inflammation and edema, on blinded histological grading by a cardiovascular pathologist (H.I-U.), as compared to the MyoC group (Fig. 3B). Hearts showed limited fibrosis in the MyoC group, and this observation was not significantly attenuated by MSC

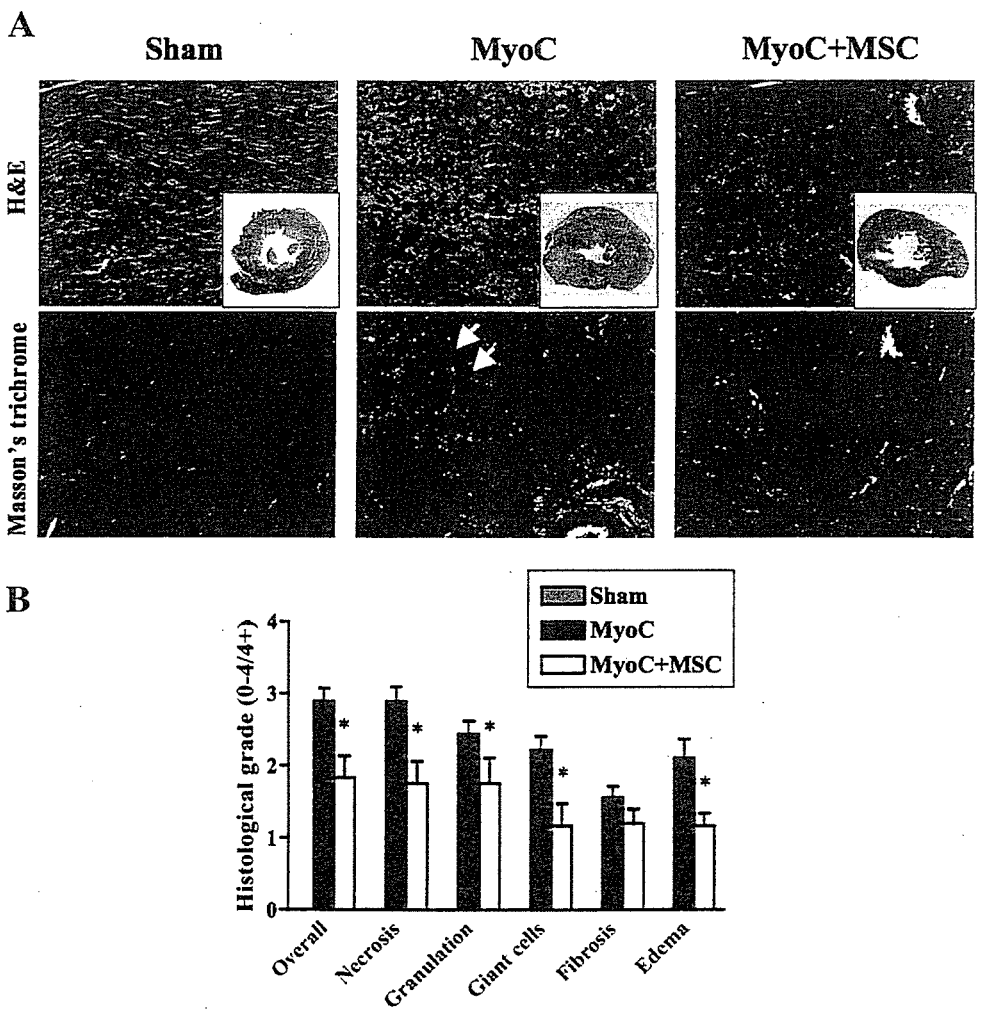

Fig. 3. Effects of MSC transplantation on pathological changes in acute myocarditis. (A) Representative myocardial sections show markedly decreased inflammation and tissue necrosis (H & E) and a comparable degree of early fibrosis (Masson's trichrome) after MSC transplantation (MyoC+MSC) as compared to control (MyoC, arrows). Insets are transverse sections of myocardium. Scale bars: 50 μm. (B) Semi-quantitative histological grades for necrosis and tissue granulation as well as for infiltration of giant cells and edema were significantly lower after MSC transplantation (MyoC+MSC) compared to control (MyoC). Sham tissues exhibited no measurable pathological change. Values are mean±S.E. *$P<0.05$ *vs* Sham, †$P<0.05$ *vs* MyoC group.

transplantation, possibly because of the acute nature of this experiment (Fig. 3B).

Notably, marked histiocytic infiltration was demonstrated by CD68-positive cells, including multinucleated giant cells, in myocarditis (MyoC group), and this was significantly attenuated by MSC transplantation (Figs. 4A and B). In myocarditis, there was an increase in MCP-1 expression localized to the vascular endothelium and also in cardiomyocytes surrounding areas of inflammation (Fig. 5A). The hearts in the MyoC+MSC group showed a partial decrease in MCP-1 expression. Serum MCP-1 level was greatly increased in the MyoC group, whereas the increase was significantly attenuated in the MyoC+MSC group (Fig. 5B).

3.3. Effect of MSC on angiogenesis

To investigate the angiogenic effect of MSC transplantation in the myocardium, immunohistochemical analysis of vWF was performed. Capillary density was increased in the MyoC group (Figs. 6A and B). Notably, in MSC-transplanted tissues, capillary density was increased compared to that in the MyoC group. The clustering of relatively small vessels seen in MSC-transplanted hearts was indicative of recent neovascularization.

3.4. Cardioprotective effects of MSC in paracrine manner

Because MSC transplantation had anti-inflammatory and tissue-protective effects and induced angiogenesis, some paracrine effects were expected. To confirm the paracrine effects of MSC *in vitro*, cardiomycytes were isolated from adult rats, and cultured with MCP-1 in the standard medium or in the conditioned medium obtained from MSC culture. The standard medium containing MCP-1 resulted in a decrease in viable cardiomyocytes; however, MSC-derived conditioned medium containing MCP-1 attenuated the decrease in viable cardiomyocytes (Fig. 7A). TUNEL staining showed that the standard medium containing MCP-1 markedly induced apoptosis of cardiomyocytes (Figs. 7B and C). However, the conditioned medium of MSC significantly attenuated MCP-1-induced cardiomyocyte apoptosis. In addition, CK activity in standard medium containing MCP-1 was significantly increased, whereas the conditioned medium markedly attenuated the CK activity induced by MCP-1 (Fig. 7D).

To investigate whether MSC secreted angiogenic and anti-fibrotic factors, VEGF and HGF levels in MSC culture were measured by ELISA assay. MSC secreted large amounts of VEGF and HGF compared to standard medium, respectively (Fig. 7E).

4. Discussion

In this study, we focused on the therapeutic potential of MSC transplantation in the acute phase of myocarditis. We showed that 1) MSC transplantation 1 week after myosin injection improved cardiac function and attenuated pathological findings including myocardial inflammation, and that 2)

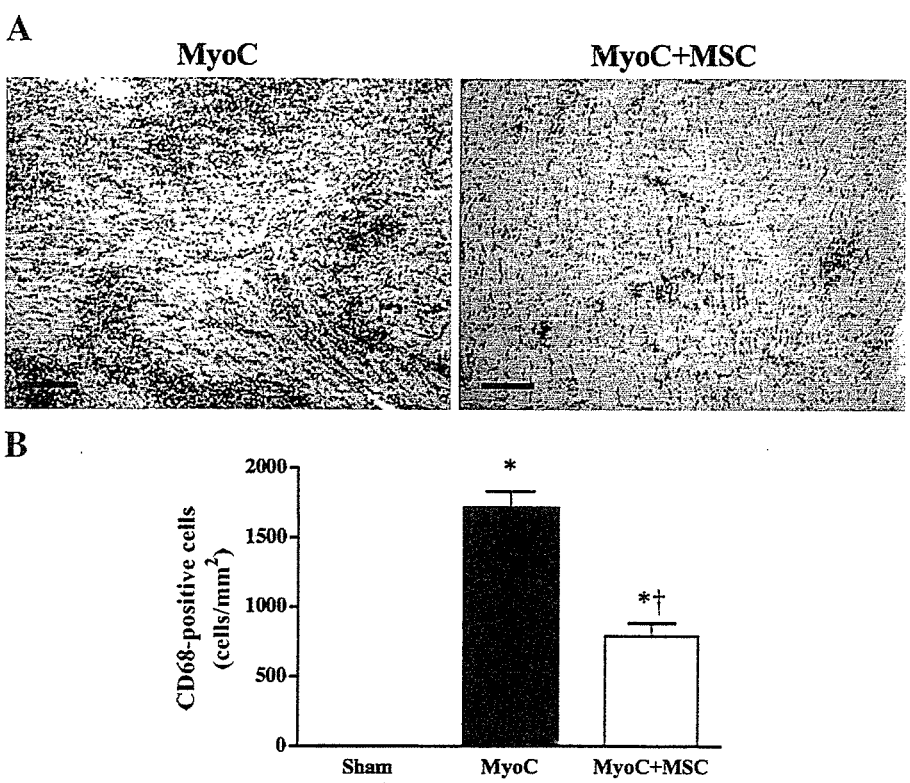

Fig. 4. Effects of MSC transplantation on myocardial CD68 expression in acute myocarditis. (A) Representative myocardial sections immunohistochemically stained for CD68 demonstrate a marked decrease in CD68-positive cells, including giant cells, after MSC transplantation (MyoC+MSC) as compared to control (MyoC). Scale bars: 100 μm. (B) Semi-quantitative counts of CD68-positive cells demonstrate a significant reduction in the MyoC+MSC group. Values are mean±S.E. *$P<0.05$ *vs* Sham, †$P<0.05$ *vs* MyoC group.

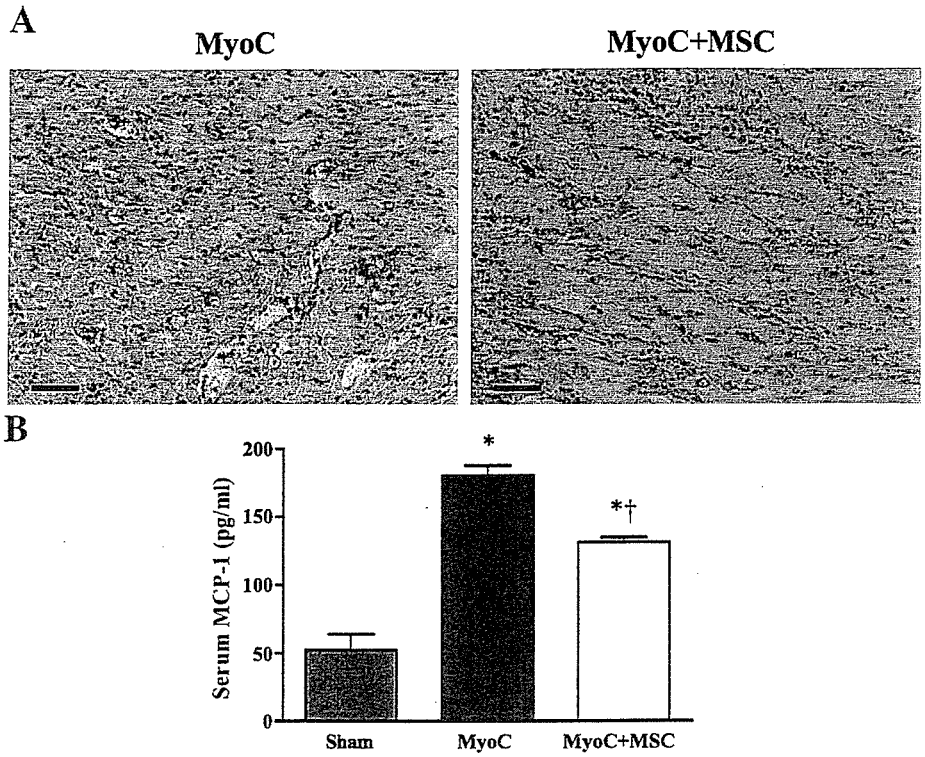

Fig. 5. Effects of MSC transplantation on myocardial MCP-1 expression and serum MCP-1 level. (A) Representative MCP-1-stained myocardial sections from MyoC and MyoC+MSC groups. Scale bars: 50 μm. (B) Serum level of MCP-1 measured by ELISA. Values are mean±S.E. *$P<0.05$ *vs* Sham, †$P<0.05$ *vs* MyoC group.

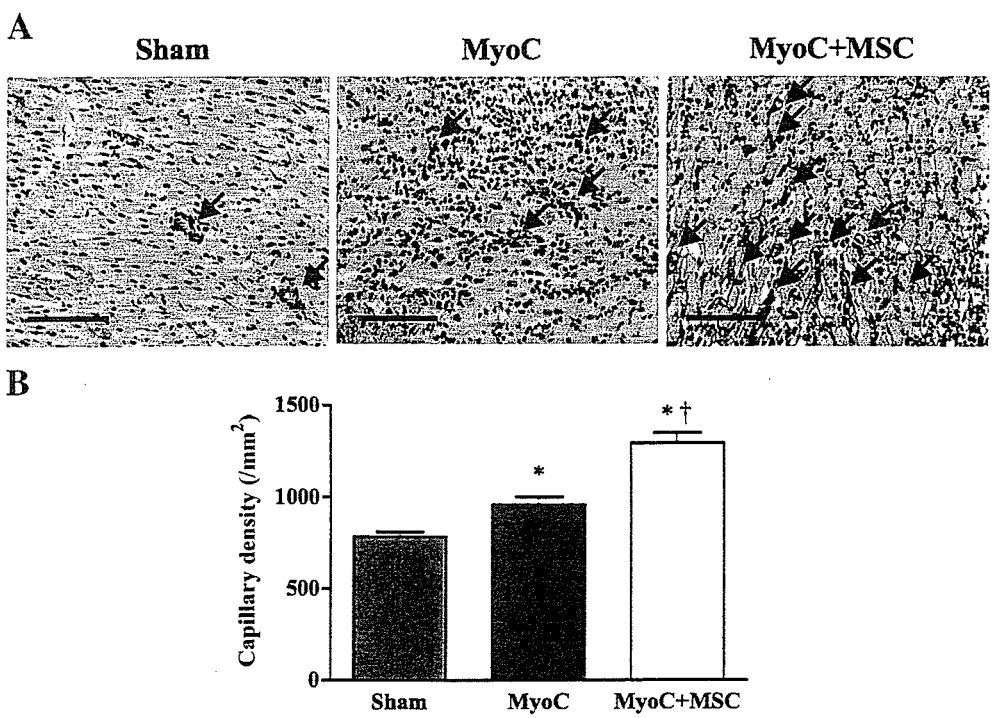

Fig. 6. Effects of MSC on neovascularization. (A) Representative myocardial sections immunohistochemically stained for vWF showing increased microvasculature (arrows) in control hearts (MyoC), which was more marked after MSC transplantation (MyoC+MSC). Scale bars: 50 μm. (B) Capillary density measured in 10 random representative high-power fields showing a significant increase in control (MyoC) and a further increase after MSC transplantation (MyoC+MSC) over the Sham group. Values are mean±S.E. *$P<0.05$ *vs* Sham, †$P<0.05$ *vs* MyoC group.

MSC had cardioprotective effects acting in a paracrine manner.

The rat model of myosin-induced experimental myocarditis provides a model that resembles human giant cell myocarditis [8,10]. Although the majority of acute myocarditis is linked to a viral infection such as coxsackievirus B3, this viral infection can in some cases cause an autoimmune myocarditis with chronic myocardial inflammation without viral persistence, due to the exposure of cardiac autoantigens to the immune system [11,12]. This myocarditis model is triphasic, consisting of an antigen priming phase from days 0–14, an autoimmune response phase from days 14–21, and a reparative phase thereafter, associated chronically with a dilated cardiomyopathy phenotype [13]. In our previous study, MSC were transplanted at the reparative

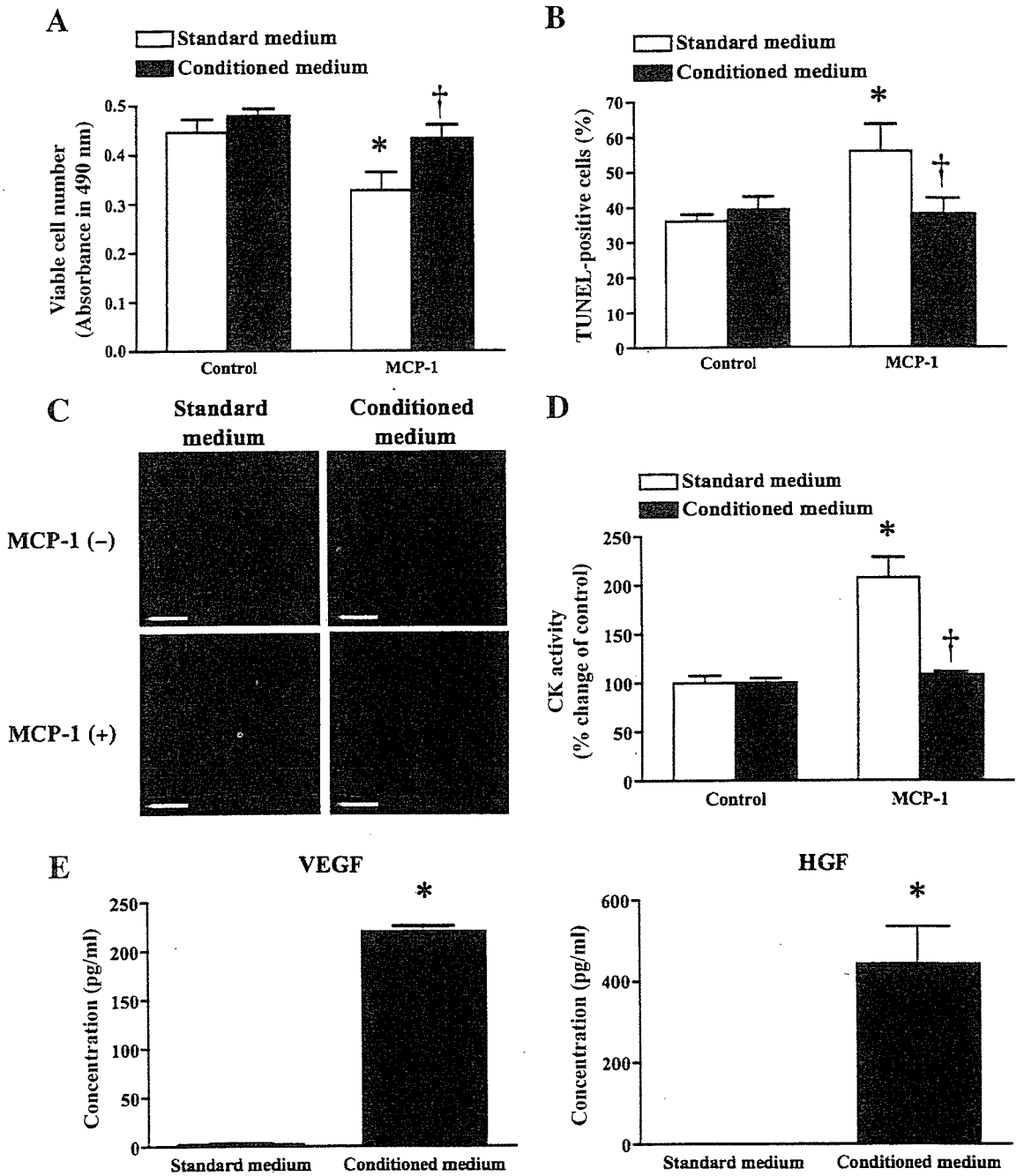

Fig. 7. Effects of MSC on MCP-1-induced cardiomyocyte injury *in vitro*. (A) MTS assay after 24 h of culture with or without MCP-1 in standard medium *vs* MSC conditioned medium. $^{*}P<0.05$ *vs* control in standard medium, $^{\dagger}P<0.05$ *vs* MCP-1 in conditioned medium. (B) Quantitative analysis of TUNEL staining after 24 h of culture with or without MCP-1 in standard medium *vs* MSC conditioned medium. $^{*}P<0.05$ *vs* control in standard medium, $^{\dagger}P<0.05$ *vs* MCP-1 in standard medium. (C) Representative TUNEL staining show increased apoptotic cardiomyocytes (green) cultured with MCP-1 in standard medium, which was attenuated by MSC conditioned medium. Nuclei were counterstained with DAPI (blue). Scale bars: 50 μm. (D) CK activity after 24 h of culture with or without MCP-1 in standard medium *vs* MSC conditioned medium. $^{*}P<0.05$ *vs* control in standard medium, $^{\dagger}P<0.05$ *vs* MCP-1 in standard medium. (E) ELISA for VEGF and HGF secreted from cultured MSC as compared to standard medium. $^{\dagger}P<0.05$ *vs* standard medium.

Physiological Significance and Therapeutic Potential of Adrenomedullin in Pulmonary Hypertension

Shinsuke Murakami[1,2], Hiroshi Kimura[2], Kenji Kangawa[3] and Noritoshi Nagaya[1,*]

[1]*Department of Regenerative Medicine and Tissue Engineering, National Cardiovascular Center Research Institute, Osaka, Japan,* [2]*Second Department of Internal Medicine, Nara Medical University, Nara, Japan,* [3]*Department of Biochemistry, National Cardiovascular Center Research Institute, Osaka, Japan*

Abstract: Adrenomedullin (ADM) is a potent vasodilator peptide that was originally isolated from human pheochromocytoma. Its vasodilatory effect is mediated by cyclic adenosine 3',5'-monophosphate- and nitric oxide-dependent mechanisms. Earlier studies have demonstrated that ADM is secreted from various tissues, including vessels, heart, and lungs. In addition, there are specific receptors for ADM in the lungs. Plasma ADM level is elevated in proportion to the severity of pulmonary hypertension, and circulating ADM is partially metabolized in the lungs. These findings suggest that ADM plays an important role in the regulation of pulmonary vascular tone. Administration of ADM by intravenous or intratracheal delivery significantly decreased pulmonary arterial pressure and pulmonary vascular resistance in patients with pulmonary arterial hypertension. Furthermore, we have recently developed a new therapeutic strategy using ADM gene-modified endothelial progenitor cells (EPC). Intravenously administered ADM gene-modified EPC were incorporated into lung tissues and attenuated monocrotaline-induced pulmonary hypertension in rats. In addition, ADM has angiogenic and anti-apoptotic activities *via* activation of Akt and/or mitogen-activated protein kinase. These findings suggest that ADM may act not only as a vasodilator but also as a vasoprotective factor. Thus, ADM may be a promising endogenous peptide for the treatment of pulmonary hypertension.

Key Words: Adrenomedullin, pulmonary hypertension, vasodilation, cyclic adenosine 3',5'-monophosphate, nitric oxide, endothelial progenitor cell, gene therapy, angiogenesis, anti-apoptosis, Akt.

INTRODUCTION

Idiopathic pulmonary arterial hypertension (IPAH) is a rare but life-threatening disease characterized by increasing pulmonary vascular resistance and progressive pulmonary hypertension that leads to right ventricular failure and death [1]. The median survival is estimated to be 2.8 years from diagnosis [2]. Because the presence of endothelial abnormalities in the pulmonary vascular bed causes pulmonary vasoconstriction, smooth muscle cell proliferation, and *in situ* thrombosis [3], a variety of vasodilators, anti-proliferative agents, and anticoagulants have been proposed as therapeutic agents for IPAH [4-6]. Despite therapeutic medical advances including prostacyclin therapy, some patients ultimately require heart-lung or lung transplantation [7,8]. Thus, a novel therapeutic strategy is desirable for the treatment of pulmonary hypertension.

Adrenomedullin (ADM), which was originally isolated from human pheochromocytoma, is a potent and long-lasting hypotensive peptide [9]. Human ADM consists of 52 amino acids with a single intramolecular disulfide bond and an amidated tyrosine at the carboxy terminus (Fig. 1) [9]. This peptide shares some structural homology with calcitonin gene-related peptide and amylin. The effects of ADM are mediated by two Gs-protein-coupled plasma membrane receptors: calcitonin-receptor-like receptor and receptor activity-modifying protein-2 or -3 [10]. Subsequent studies have revealed that immunoreactive ADM is distributed in plasma and a wide range of tissues including aorta, ventricles, lungs, and kidneys [11,12]. In particular, ADM is actively produced and secreted by vascular endothelial cells and vascular smooth muscle cells [13-15]. In addition to potent vasodilating effects, ADM has been reported to have multiple effects on cardiovascular and renal function, such as diuretic and natriuretic effects [16,17], and a positive inotropic effect [18,19]. Recently, ADM has received much attention as an important factor in cell growth and survival [20-25]. Thus, ADM has come to be regarded as a multifunctional peptide.

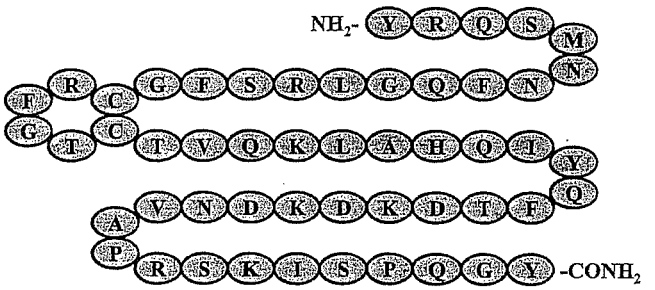

Fig. (1). Human adrenomedullin consists of 52 amino acids with a single intramolecular disulfide bond between residues 16 and 21 and with an amidated tyrosine at the carboxy terminus.

Previous studies have shown that plasma and/or tissue ADM levels are elevated in a variety of cardiovascular and renal diseases including hypertension [26-28], acute myocardial infarction [29-32], heart failure [33-39], and renal failure [40]. We and others have reported that plasma

*Address correspondence to this author at the Department of Regenerative Medicine and Tissue Engineering, National Cardiovascular Center Research Institute, 5-7-1 Fujishirodai, Suita, Osaka 565-8565, Japan; Tel: +81-6-6833-5012; Fax: +81-6-6872-7485; E-mail: nnagaya@ri.ncvc.go.jp

1871-529X/06 $50.00+.00

ADM levels are also elevated in patients with pulmonary hypertension in proportion to the clinical severity [41-43]. These findings suggest that ADM may be involved in the regulation of cardiovascular and renal function and vascular tone. Recent studies have reported that in heterozygous ADM knockout mice with almost half the level of ADM in organs and plasma, marked cardiac hypertrophy and coronary artery lesions were observed under conditions of high cardiovascular stress [44,45]. Thus, endogenous ADM may possess a protective effect against cardiovascular damage, and increased plasma and/or tissue ADM levels may be a compensatory response to organ failure.

This review summarizes the physiological significance of ADM in patients with pulmonary hypertension and the therapeutic potential of ADM for the treatment of pulmonary hypertension.

PLASMA LEVELS OF ADRENOMEDULLIN IN PATIENTS WITH PULMONARY HYPERTENSION

Plasma ADM levels have been reported to be elevated in patients with pulmonary arterial hypertension [46] and in animal models of experimental pulmonary hypertension induced by monocrotaline [47]. To investigate the pathophysiological significance of ADM in pulmonary hypertension, we studied the relationship between plasma ADM levels and pulmonary hemodynamics in patients with pulmonary arterial hypertension [41]. Plasma ADM levels in patients with pulmonary arterial hypertension were significantly higher than those in healthy subjects. In addition, there were significant correlations between the plasma ADM level and mean pulmonary arterial pressure, total pulmonary resistance, and mean right arterial pressure. These findings suggest that the plasma ADM level is increased in proportion to the severity of pulmonary hypertension and right heart failure.

Previous studies have shown that ADM mRNA and its receptor mRNA are highly expressed in the lung [48]. Yoshibayashi *et al.* measured plasma ADM levels in blood samples obtained from various sites during cardiac catheterization in patients with pulmonary hypertension [46]. The plasma ADM level in the pulmonary vein was significantly lower than that in the pulmonary artery, consistent with the previous finding that the pulmonary circulation is the site of ADM clearance [49]. These findings suggest that elevated endogenous ADM in plasma may play an important role in the pulmonary circulation.

Previous studies have demonstrated that hypoxia, cytokine production, and shear stress induce ADM secretion by vascular cells [50-52]. An *in vitro* study has demonstrated that ADM is upregulated through a hypoxia-inducible factor-1 (HIF-1)-dependent pathway under hypoxic conditions [53]. Thus, hypoxia/HIF-1 is one of the most potent regulators of ADM production in pulmonary arterial hypertension.

BIOLOGICAL ACTIONS OF ADRENOMEDULLIN

Intravenous infusion of ADM results in potent and sustained hypotension [17,44,54,55]. ADM has been shown to increase the intracellular cyclic adenosine 3',5'-monophosphate (cAMP) level in vascular smooth muscle cells *via* its specific receptor [56,57]. The increase in cAMP by ADM activates protein kinase A (PKA), resulting in a decrease in calcium content in smooth muscle cells. On the other hand, ADM has been shown to induce vasorelaxation in a nitric oxide (NO)-dependent manner [58]. ADM induces activation of endothelial NO synthase in vascular endothelial cells *via* the Ca^{2+}/calmodulin-dependent [59] and the phosphatidylinositol 3-kinase (PI3K)/Akt-dependent pathway [60]. Thus, ADM regulates vascular tone through a cAMP-dependent mechanism and/or a NO-dependent mechanism (Fig. 2). It has been reported that there are many binding sites for ADM in the lung [61] and that ADM preferentially dilates pulmonary arterial resistance vessels [62]. These findings raise the possibility that ADM may play an important role in the regulation of pulmonary vascular tone in patients with pulmonary hypertension.

An imbalance between vasodilators and vasoconstrictors has been thought to have a key role in the development of IPAH [63]. Endothelial dysfunction decreases the production of vasodilators such as prostacyclin and NO, whereas it increases that of vasoconstrictors including thromboxane and endothelin-1 [3]. Previous studies demonstrated that prostacyclin synthase [64] and endothelial nitric oxide synthase [65] expression were decreased in the lungs of patients with pulmonary hypertension. Thus, pulmonary endothelial cells may be a therapeutic target for the treatment of pulmonary hypertension. ADM regulates growth and survival of endothelial cells [22,66,67]. ADM signaling is of particular significance in endothelial biology, since the peptide protects cells from apoptosis and promotes angiogenesis at least in part through activation of PI3K/Akt and mitogen-activated protein kinase/extracellular signal-regulated kinase 1/2 in endothelial cells. These findings raise the possibility that elevated plasma ADM in patients with pulmonary hypertension may exert protective effects on pulmonary endothelial cells.

Plexiform lesions, the classic pathological finding in IPAH, are present in about one in three lung biopsy specimens [68]. These lesions have been considered an abnormal growth of modified smooth muscle cells [69]. *In vitro*, ADM has been shown to inhibit serum or platelet-derived growth factor-stimulated proliferation and migration in smooth muscle cells [70-72]. *In vivo*, continuous infusion of ADM has been shown to inhibit pulmonary smooth muscle cell proliferation in monocrotaline-induced pulmonary hypertension in rats [73]. These results suggest that ADM may have an inhibitory function in pulmonary vascular remodeling.

The overproduction of reactive oxygen species results in the progression of pulmonary vascular remodeling. ADM is recognized as a potent antioxidant. An *in vitro* study showed ADM suppressed reactive oxygen species production in a dose-dependent manner *via* activation of the cAMP-protein kinase A pathway [74]. Heterozygous ADM knockout mice housed under hypoxia showed not only severe pulmonary vascular injury but also higher levels of reactive oxygen species production [75]. These findings suggest that ADM might be one of the important compensatory substances to protect against hypoxia-induced pulmonary vascular remodeling, possibly through the suppression of reactive oxygen species.

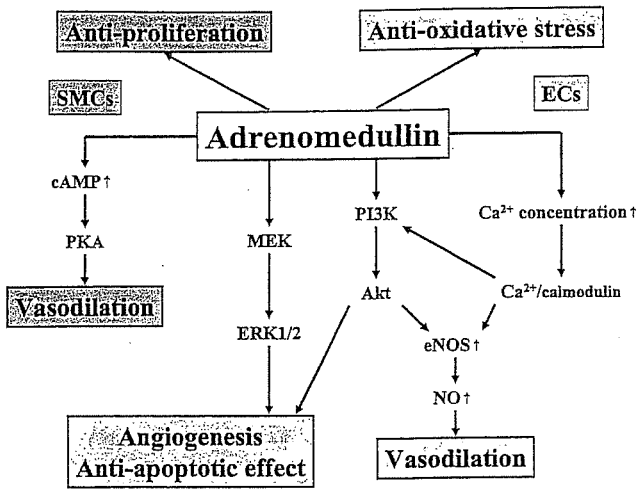

Fig. (2). Signaling pathway of adrenomedullin (ADM) in vascular endothelial cells (ECs) and smooth muscle cells (SMCs). ADM regulates vascular tone through a cAMP-dependent mechanism and/or a NO-dependent mechanism. ADM protects cells from apoptosis and promotes angiogenesis at least in part through activation of Akt and ERK1/2 in endothelial cells. ADM also inhibits smooth muscle cell proliferation and suppresses reactive oxygen species production.

THERAPEUTIC POTENTIAL OF ADRENOMEDULLIN IN PULMONARY HYPERTENSION

Previous experimental studies have shown that exogenously administered ADM causes a dose-related decrease in pulmonary arterial pressure under conditions of high pulmonary vascular tone [62,76,77]. Short-term infusion of ADM attenuates pulmonary hypertension secondary to congestive heart failure [78,79], and long-term infusion of ADM attenuates progressive pulmonary hypertension and medial thickening of the pulmonary arteries in rats treated with monocrotaline [73]. However, in humans, it remains unknown whether exogenous ADM has beneficial effects in patients with precapillary pulmonary hypertension such as IPAH or chronic thromboembolic pulmonary hypertension. Accordingly, we examined the hemodynamic and hormonal responses to intravenous infusion of ADM or placebo in 13 patients with precapillary pulmonary hypertension [80]. ADM (0.05μg/kg/minute) or placebo was randomly administered at a rate of 0.5 ml/minute for 30 minutes. At the end of ADM infusion, plasma ADM level was increased about 3-fold in the ADM group. ADM infusion produced a 44% increase in cardiac index and a 32% decrease in pulmonary vascular resistance, and its hemodynamic effects lasted at least 15 minutes after the end of infusion. These results suggest that ADM has potent, relatively long-lasting pulmonary vasodilator activity in patients with pulmonary hypertension. We have shown that plasma cAMP level was increased by 23% during ADM infusion. The increase in cAMP by ADM activates PKA, resulting in a decrease in calcium content in smooth muscle cells [57]. It is therefore possible that ADM may relax vascular smooth muscle by inducing an increase in cAMP level. ADM infusion markedly increased the cardiac index in patients with pulmonary hypertension. Considering the strong vasodilator activity of ADM in the systemic and pulmonary vasculature, a significant decrease in cardiac afterload may be responsible for the increased cardiac index with ADM. On the other hand, a previous binding study has shown abundant, specific binding sites for ADM in ventricular myocardium [61]. ADM has been shown to increase cardiac cAMP [81,82], which is known to mediate the positive inotropic action of beta-adrenergic stimulation. Alternatively, ADM has been shown to produce a positive inotropic action through cAMP-independent mechanisms [83]. These findings suggest that the increase in cardiac index may be attributable not only to a fall in cardiac afterload but also to the direct positive inotropic action of ADM. Further studies are necessary to investigate the therapeutic potential and safety of ADM in patients with pulmonary hypertension.

Intravenously administered ADM decreased systemic vascular resistance and induced systemic hypotension in patients with pulmonary hypertension because of nonselective vasodilation in the pulmonary and systemic vascular beds. Recently, inhalation of aerosolized prostacyclin and its analogue, iloprost, has been shown to cause pulmonary vasodilation without systemic hypotension in patients with IPAH [84,85]. In addition, inhalant application of vasodilators does not impair gas exchange because the ventilation-matched deposition of drug in the alveoli causes pulmonary vasodilation matched to ventilated areas. In clinical settings, inhalation therapy may be more simple, noninvasive, and comfortable than continuous intravenous infusion therapy. These findings raise the possibility that ADM inhalation may have beneficial effects in patients with precapillary pulmonary hypertension. We examined the effects of ADM inhalation on monocrotaline-induced pulmonary hypertension in rats [86]. ADM (5 μg/kg) or saline was inhaled as an aerosol using an ultrasonic nebulizer. To assess the acute effect of inhaled ADM, hemodynamic studies were carried out at 3 weeks after monocrotaline injection. Expectedly, a single 30-minute inhalation of ADM significantly decreased total pulmonary vascular resistance without a significant decrease in mean arterial pressure in rats given monocrotaline. These hemodynamic effects of ADM lasted at least 60

minutes after the end of inhalation. Furthermore, to assess the chronic effect of inhaled ADM, 30-minute inhalation of ADM or saline was repeated four times a day for 3 weeks after monocrotaline injection. Repeated inhalation of ADM markedly decreased mean pulmonary arterial pressure and total pulmonary vascular resistance without systemic hypotension in rats given monocrotaline. Interestingly, repeated inhalation of ADM significantly attenuated an increase in medial wall thickness of peripheral pulmonary arteries and improved survival. Considering the potent vasoprotective effects of ADM such as vasodilation and inhibition of smooth muscle cell migration and proliferation, it is interesting to speculate that ADM trapped in the bronchial epithelium or alveoli leaks to the pulmonary arteries to maintain pulmonary vascular integrity in rats given monocrotaline. von der Hardt *et al.* have reported that aerosolized ADM (6 μg/kg) resulted in a sustained reduction in mean pulmonary arterial pressure in a surfactant-depleted piglet model [87]. There was no significant difference in mean systemic arterial pressure after ADM inhalation. Interestingly, they reported that aerosolized ADM reduced endothelin (ET)-1 mRNA in lung tissue and ET-1 protein expression in pulmonary arteries. ET-1 is a potent pulmonary vasoconstrictor [88] and plays an important role in pulmonary hypertension [89-93]. Thus, reduction of ET-1 expression may contribute to the effect of aerosolized ADM on pulmonary hypertension. Recently, we have investigated the effects of ADM inhalation on pulmonary hemodynamics and exercise capacity in patients with IPAH [94]. Inhalation of aerosolized ADM (10 μg/kg) produced a 22% decrease in pulmonary vascular resistance. However, neither systemic arterial pressure nor heart rate was altered. These results suggest that inhaled ADM improves hemodynamics with pulmonary selectivity. In addition, inhalation of ADM improved exercise capacity, as indicated by increased peak oxygen consumption during exercise. Although further studies are necessary to maximize the efficiency and reproducibility of pulmonary ADM delivery, inhalation of ADM may be a promising approach to treat pulmonary hypertension without affecting the systemic circulation.

Recently, stem or progenitor cell transplantation has received much attention as a novel therapeutic option to regenerate a variety of tissues. In 1997, Asahara *et al.* isolated endothelial progenitor cells (EPC) from human peripheral blood [95]. EPC are mobilized from bone marrow into the peripheral blood in response to tissue ischemia or traumatic injury, migrate to sites of injured endothelium, and differentiate into mature endothelial cells *in situ* [96-98]. Transplantation of EPC has been shown to induce therapeutic angiogenesis in the ischemic heart or limb [99-101]. We have shown that intravenously administered EPC are incorporated into the pulmonary vasculature and attenuate pulmonary hypertension in the rat monocrotaline model of IPAH [102]. Thus, the regeneration of pulmonary vascular endothelium by cell transplantation may be a new therapeutic strategy for the treatment of pulmonary hypertension. A recent study has reported that human telomerase reverse transcriptase gene transfer enhances the angiogenic properties of EPC [103]. Considering the variety of protective effects of ADM on vascular endothelial cells, we hypothesized that ADM gene transfer into EPC may strengthen their therapeutic potential. Recently, Fukunaka *et al.* have developed a nonviral vector, gelatin hydrogel [104,105]. Positively charged gelatin can hold negatively charged plasmid DNA in its lattice structure. DNA-gelatin complexes can delay gene degradation, leading to efficient gene transfer [106,107]. Interestingly, EPC phagocytose ionically linked DNA-gelatin complexes in coculture, which allows nonviral gene transfer into EPC with high efficiency. ADM gene transfer into EPC inhibits cell apoptosis and induces proliferation and migration, suggesting that ADM gene transfer strengthens the therapeutic potential of EPC. Furthermore, genetically modified EPCs markedly secreted ADM peptide and ADM overproduction lasted for more than 16 days. Therefore, transplanted EPC may serve not only as a tissue-engineering tool to reconstruct the pulmonary vasculature but also as a vehicle for gene delivery to injured pulmonary endothelium. We have investigated whether cell (EPC)-based ADM gene transfer causes further improvement in monocrotaline-induced pulmonary hypertension in rats [102]. ADM gene-modified EPC were similarly incorporated into the pulmonary vasculature, and significantly decreased pulmonary vascular resistance compared with EPC alone. A single transplantation of ADM gene-modified EPC improved survival in monocrotaline rats compared with transplantation of EPC alone. Thus, a novel hybrid cell-gene therapy may be a new therapeutic strategy for the treatment of pulmonary hypertension including IPAH. However, the initial success of gelatin-mediated ADM gene therapy reported here should be confirmed by long-term experiments, and extensive toxicity studies in animals are needed before clinical trials.

SUMMARY

This article describes the physiological significance of ADM and its therapeutic potential for the treatment of pulmonary hypertension. ADM has been shown to possess a variety of actions, including vasodilatory actions, regulation of cell growth and survival, and modulation of hormone secretion. Plasma ADM levels are elevated in patients with pulmonary hypertension in proportion to the clinical severity, and circulating ADM is partially metabolized in the lungs. Nevertheless, exogenously administered ADM induces hemodynamic improvement. These findings suggest that ADM may be a promising therapeutic agent for the treatment of pulmonary hypertension including IPAH. Further studies are necessary to evaluate the long-term efficacy and safety of ADM in patients with pulmonary hypertension.

ABBREVIATIONS

ADM = Adrenomedullin

cAMP = Cyclic adenosine 3',5'-monophosphate

EPC = Endothelial progenitor cell

ET = Endothelin

IPAH = Idiopathic pulmonary arterial hypertension

NO = Nitric oxide

PI3K = Phosphatidylinositol 3-kinase

PKA = Protein kinase A

REFERENCES

[1] Rich, S., Dantzker, D.R., Ayres, S.M., Bergofsky, E.H., Brundage, B.H., Detre, K.M., Fishman, A.P., Goldring, R.M., Groves, B.M., Koerner, S.K. Primary pulmonary hypertension. A national prospective study. *Ann. Intern. Med.*, **1987**, *107*, 216-223.

[2] D'Alonzo, G.E., Barst, R.J., Ayres, S.M., Bergofsky, E.H., Brundage, B.H., Detre, K.M., Fishman, A.P., Goldring, R.M., Groves, B.M., Kernis, J.T. Survival in patients with primary pulmonary hypertension. Results from a national prospective registry. *Ann. Intern. Med.*, **1991**, *115*, 343-349.

[3] Archer, S., Rich, S. Primary pulmonary hypertension: a vascular biology and translational research "Work in progress". *Circulation*, **2000**, *102*, 2781-2791.

[4] Barst, R.J., Rubin, L.J., Long, W.A, McGoon, M.D., Rich, S., Badesch, D.B., Groves, B.M., Tapson, V.F., Bourge, R.C., Brundage, B.H. A comparison of continuous intravenous epoprostenol (prostacyclin) with conventional therapy for primary pulmonary hypertension. The Primary Pulmonary Hypertension Study Group. *N. Engl. J. Med.*, **1996**, *334*, 296-302.

[5] McLaughlin, V.V., Genthner, D.E., Panella, M.M., Rich, S. Reduction in pulmonary vascular resistance with long-term epoprostenol (prostacyclin) therapy in primary pulmonary hypertension. *N. Engl. J. Med.*, **1998**, *338*, 273-277.

[6] Rubin, L.J., Mendoza, J., Hood, M., McGoon, M., Barst, R., Williams, W.B., Diehl, J.H., Crow, J., Long, W. Treatment of primary pulmonary hypertension with continuous intravenous prostacyclin (epoprostenol). Results of a randomized trial. *Ann. Intern. Med.*, **1990**, *112*, 485-491.

[7] Reitz, B.A., Wallwork, J.L., Hunt, S.A., Pennock, J.L., Billingham, M.E., Oyer, P.E., Stinson, E.B., Shumway, N.E. Heart-lung transplantation: successful therapy for patients with pulmonary vascular disease. *N. Engl. J. Med.*, **1982**, *306*, 57-64.

[8] Pasque, M.K., Trulock, E.P., Kaiser, L.R, Cooper, J.D. Single-lung transplantation for pulmonary hypertension. Three-month hemodynamic follow-up. *Circulation*, **1991**, *84*, 2275-2279.

[9] Kitamura, K., Kangawa, K., Kawamoto, M., Ichiki, Y., Nakamura, S., Matsuo, H., Eto, T. Adrenomedullin: a novel hypotensive peptide isolated from human pheochromocytoma. *Biochem. Biophys. Res. Commun.*, **1993**, *192*, 553-560.

[10] McLatchie, L.M., Fraser, N.J., Main, M.J., Wise, A., Brown, J., Thompson, N., Solari, R., Lee, M.G., Foord, S.M. RAMPs regulate the transport and ligand specificity of the calcitonin-receptor-like receptor. *Nature*, **1998**, *393*, 333-339.

[11] Ichiki, Y., Kitamura, K., Kangawa, K., Kawamoto, M., Matsuo, H., Eto, T. Distribution and characterization of immunoreactive adrenomedullin in human tissue and plasma. *FEBS Lett.*, **1994**, *338*, 6-10.

[12] Sakata, J., Shimokubo, T., Kitamura, K., Nishizono, M., Iehiki, Y., Kangawa, K., Matsuo, H., Eto, T. Distribution and characterization of immunoreactive rat adrenomedullin in tissue and plasma. *FEBS Lett.*, **1994**, *352*, 105-108.

[13] Shimekake, Y., Nagata, K., Ohta, S., Kambayashi, Y., Teraoka, H., Kitamura, K., Eto, T., Kangawa, K., Matsuo, H. Adrenomedullin stimulates two signal transduction pathways, cAMP accumulation and Ca^{2+} mobilization, in bovine aortic endothelial cells. *J. Biol. Chem.*, **1995**, *270*, 4412-4417.

[14] Sugo, S., Minamino, N., Kangawa, K., Miyamoto, K., Kitamura, K., Sakata, J., Eto, T., Matsuo, H. Endothelial cells actively synthesize and secrete adrenomedullin. *Biochem Biophys. Res. Commun.*, **1994**, *201*, 1160-1166.

[15] Sugo, S., Minamino, N., Shoji, H., Kangawa, K., Kitamura, K., Eto, T., Matsuo, H. Production and secretion of adrenomedullin from vascular smooth muscle cells: augmented production by tumor necrosis factor-alpha. *Biochem. Biophys. Res. Commun.*, **1994**, *203*, 719-726.

[16] Majid, D.S., Kadowitz, P.J., Coy, D.H., Navar, L.G. Renal responses to intra-arterial administration of adrenomedullin in dogs. *Am .J .Physiol.*, **1996**, *270*, F200-F205.

[17] Parkes, D.G., May, C.N. Direct cardiac and vascular actions of adrenomedullin in conscious sheep. *Br. J. Pharmacol.*, **1997**, *120*, 1179-1185.

[18] Szokodi, I., Kinnunen, P., Tavi, P., Weckstrom, M., Toth, M., Ruskoaho, H. Evidence for cAMP-independent mechanisms mediating the effects of adrenomedullin, a new inotropic peptide. *Circulation*, **1998**, *97*, 1062-70.

[19] Nagaya, N., Goto, Y., Satoh, T., Sumida, H., Kojima, S., Miyatake, K., Kangawa, K. Intravenous adrenomedullin in myocardial function and energy metabolism in patients after myocardial infarction. *J. Cardiovasc. Pharmacol.*, **2002**, *39*, 754-760.

[20] Kato, H., Shichiri, M., Marumo, F., Hirata, Y. Adrenomedullin as an autocrine/paracrine apoptosis survival factor for rat endothelial cells. *Endocrinology*, **1997**, *138*, 2615-2620.

[21] Nagaya, N., Mori, H., Murakami, S., Kangawa, K., Kitamura, S. Adrenomedullin: angiogenesis and gene therapy. *Am. J. Physiol. Regul. Integr. Comp .Physiol.*, (in press).

[22] Hanabusa, K., Nagaya, N., Iwase, T., Itoh, T., Murakami, S., Shimizu, Y., Taki, W., Miyatake, K., Kangawa, K. Adrenomedullin enhances therapeutic potency of mesenchymal stem cells after experimental stroke in rats. *Stroke*. **2005**, *36*, 853-858.

[23] Iwase, T., Nagaya, N., Fujii, T., Itoh, T., Ishibashi-Ueda, H., Yamagishi, M., Miyatake, K., Matsumoto, T., Kitamura, S., Kangawa, K. Adrenomedullin enhances angiogenic potency of bone marrow transplantation in a rat model of hindlimb ischemia. *Circulation*, **2005**, *111*, 356-362.

[24] Fujii, T., Nagaya, N., Iwase, T., Murakami, S., Miyahara, Y., Nishigami, K., Ishibashi-Ueda H., Shirai, M., Itoh, T., Ishino, K., Sano, S., Kangawa, K., Mori, H. Adrenomedullin enhances therapeutic potency of bone marrow transplantation for myocardial infarction in rats. *Am. J. Physiol. Heart. Circ. Physiol.*, **2005**, *288*, H1444-H1450.

[25] Okumura, H., Nagaya, N., Itoh, T., Okano, I., Hino, J., Mori, K., Tsukamoto, Y., Ishibashi-Ueda, H., Miwa, S., Tambara, K., Toyokuni, S., Yutani, C., Kangawa, K. Adrenomedullin infusion attenuates myocardial ischemia/reperfusion injury through the phosphatidylinositol 3-kinase/Akt-dependent pathway. *Circulation*, **2004**, *109*, 242-248.

[26] Kohno, M., Hanehira, T., Kano, H., Horio, T., Yokokawa, K., Ikeda, M., Minami, M., Yasunari, K., Yoshikawa, J. Plasma adrenomedullin concentrations in essential hypertension. *Hypertension*, **1996**, *27*, 102-107.

[27] Nishikimi, T., Yoshihara, F., Kanazawa, A., Okano, I., Horio, T., Nagaya, N., Yutani, C., Matsuo, H., Matsuoka, H., Kangawa, K. Role of increased circulating and renal adrenomedullin in rats with malignant hypertension. *Am. J. Physiol. Regul. Integr. Comp. Physiol.*; **2001**, *281*, R2079-R2087.

[28] Nishikimi, T., Horio, T., Kohmoto, Y., Yoshihara, F., Nagaya, N., Inenaga, T., Saito, M., Teranishi, M., Nakamura, M., Ohrui, M., Kawano, Y., Matsuo, H., Ishimitsu, T., Takishita, S., Matsuoka, H., Kangawa, K. Molecular forms of plasma and urinary adrenomedullin in normal, essential hypertension and chronic renal failure. *J. Hypertens.*, **2001**, *19*, 765-773.

[29] Kobayashi, K., Kitamura, K., Hirayama, N., Date, H., Kashiwagi, T., Ikushima, I., Hanada, Y., Nagatomo, Y., Takenaga, M., Ishikawa, T., Imamura, T., Koiwaya, Y., Eto, T. Increased plasma adrenomedullin in acute myocardial infarction. *Am .Heart J.*, **1996**, *131*, 676-680.

[30] Miyao, Y., Nishikimi, T., Goto, Y., Miyazaki, S., Daikoku, S., Morii, I., Matsumoto, T., Takishita, S., Miyata, A., Matsuo, H., Kangawa, K., Nonogi, H. Increased plasma adrenomedullin levels in patients with acute myocardial infarction in proportion to the clinical severity. *Heart*, **1998**, *79*, 39-44.

[31] Nagaya, N., Nishikimi, T., Yoshihara, F., Horio, T., Morimoto, A., Kangawa, K. Cardiac adrenomedullin gene expression and peptide accumulation after acute myocardial infarction in rats. *Am. J. Physiol. Regul. Integr. Comp. Physiol.*, **2000**, *278*, R1019-R1026.

[32] Nagaya, N., Nishikimi, T., Uematsu, M., Yoshitomi, Y., Miyao, Y., Miyazaki, S., Goto, Y., Kojima, S., Kuramochi, M., Matsuo, H., Kangawa, K., Nonogi, H. Plasma adrenomedullin as an indicator of prognosis after acute myocardial infarction. *Heart*, **1999**, *81*, 483-487.

[33] Jougasaki, M., Wei, C.M., McKinley, L.J., Burnett, J.C.Jr., Elevation of circulating and ventricular adrenomedullin in human congestive heart failure. *Circulation*, **1995**, *92*, 286-289.

[34] Nishikimi, T., Saito, Y., Kitamura, K., Ishimitsu, T., Eto, T., Kangawa, K., Matsuo, H., Omae, T., Matsuoka, H. Increased plasma levels of adrenomedullin in patients with heart failure. *J. Am. Coll .Cardiol.*, **1995**, *26*, 1424-1431.

[35] Watanabe, K., Nishikimi, T., Takamuro, M., Yasuda, K., Ishikawa, Y., Tanabe, S., Yamada, O., Nagaya, N., Matsuoka, H., Kangawa, K., Echigo, S. Two molecular forms of adrenomedullin in congenital heart disease. *Pediatr. Cardiol.*, **2003**, *24*, 559-565.

[36] Tambara, K., Fujita, M., Nagaya, N., Miyamoto, S., Iwakura, A., Doi, K., Sakaguchi, G., Nishimura, K., Kangawa, K., Komeda, M. Increased pericardial fluid concentrations of the mature form of adrenomedullin in patients with cardiac remodelling. *Heart,* **2002**, *87*, 242-246.

[37] Yoshihara, F., Nishikimi, T., Horio, T., Yutani, C., Nagaya ,N., Matsuo, H., Ohe, T., Kangawa, K. Ventricular adrenomedullin concentration is a sensitive biochemical marker for volume and pressure overload in rats. *Am. J. Physiol. Heart. Circ. Physiol.*, **2000**, *278*, H633-H642.

[38] Morimoto, A., Nishikimi, T., Yoshihara, F., Horio, T., Nagaya, N., Matsuo, H., Dohi, K., Kangawa, K. Ventricular adrenomedullin levels correlate with the extent of cardiac hypertrophy in rats. *Hypertension,* **1999**, *33*, 1146-1152.

[39] Nagaya, N., Nishikimi, T., Horio, T., Yoshihara, F., Kanazawa, A., Matsuo, H., Kangawa, K. Cardiovascular and renal effects of adrenomedullin in rats with heart failure. *Am. J. Physiol.*, **1999**, *276*, R213-R218.

[40] Ishimitsu, T., Nishikimi, T., Saito, Y., Kitamura, K., Eto, T., Kangawa, K., Matsuo, H., Omae, T., Matsuoka, H. Plasma levels of adrenomedullin, a newly identified hypotensive peptide, in patients with hypertension and renal failure. *J. Clin. Invest.*, **1994**, *94*, 2158-2161.

[41] Kakishita, M., Nishikimi, T., Okano, Y., Satoh, T., Kyotani, S., Nagaya, N., Fukushima, K., Nakanishi, N., Takishita, S., Miyata, A., Kangawa, K., Matsuo, H., Kunieda, T. Increased plasma levels of adrenomedullin in patients with pulmonary hypertension. *Clin. Sci., (Lond)* **1999**, *96*, 33-39.

[42] Vijay, P., Szekely, L., Sharp, T.G., Miller, A., Bando, K., Brown, J.W. Adrenomedullin in patients at high risk for pulmonary hypertension. *Ann. Thorac. Surg.*, **1998**, *66*, 500-505.

[43] Nishikimi, T., Nagata, S., Sasaki, T., Yoshihara, F., Nagaya, N., Horio, T., Matsuo, H., Matsuoka, H., Kangawa, K. The active molecular form of plasma adrenomedullin is extracted in the pulmonary circulation in patients with mitral stenosis: possible role of adrenomedullin in pulmonary hypertension. *Clin. Sci (Lond).*, **2001**, *100*, 61-66.

[44] Shimosawa, T., Shibagaki, Y., Ishibashi, K., Kitamura, K., Kangawa, K., Kato, S., Ando, K., Fujita, T. Adrenomedullin, an endogenous peptide, counteracts cardiovascular damage. *Circulation,* **2002**, *105*, 106-111.

[45] Niu, P., Shindo, T., Iwata, H., Iimuro, S., Takeda, N., Zhang, Y., Ebihara, A., Suematsu, Y., Kangawa, K., Hirata, Y., Nagai, R. Protective effects of endogenous adrenomedullin on cardiac hypertrophy, fibrosis, and renal damage. *Circulation,* **2004**, *109*, 1789-1794.

[46] Yoshibayashi, M., Kamiya, T., Kitamura, K., Saito, Y., Kangawa, K., Nishikimi, T., Matsuoka, H., Eto, T., Matsuo, H. Plasma levels of adrenomedullin in primary and secondary pulmonary hypertension in patients <20 years of age. *Am. J. Cardiol.*, **1997**, *79*, 1556-1558.

[47] Shimokubo, T., Sakata, J., Kitamura, K., Kangawa, K., Matsuo, H., Eto, T. Augmented adrenomedullin concentrations in right ventricle and plasma of experimental pulmonary hypertension. *Life Sci.*, **1995**, *57*, 1771-1779.

[48] Kitamura, K., Sakata, J., Kangawa, K., Kojima, M., Matsuo, H., Eto, T. Cloning and characterization of cDNA encoding a precursor for human adrenomedullin. *Biochem. Biophys. Res. Commun.*, **1993**, *194*, 720-725.

[49] Nishikimi, T., Kitamura, K., Saito, Y., Shimada, K., Ishimitsu, T., Takamiya, M., Kangawa, K., Matsuo, H., Eto, T., Omae, T. Clinical studies on the sites of production and clearance of circulating adrenomedullin in human subjects. *Hypertension,* **1994**, *24*, 600-604.

[50] Nakayama, M., Takahashi, K., Murakami, O., Shirato, K., Shibahara, S. Induction of adrenomedullin by hypoxia and cobalt chloride in human colorectal carcinoma cells. *Biochem. Biophys. Res. Commun.*, **1998**, *243*, 514-517.

[51] Sugo, S., Minamino, N., Shoji, H., Kangawa, K., Kitamura, K., Eto, T., Matsuo, H. Interleukin-1, tumor necrosis factor and lipopolysaccharide additively stimulate production of adrenomedullin in vascular smooth muscle cells. *Biochem. Biophys. Res. Commun.*, **1995**, *207*, 25-32.

[52] Chun, T.H., Itoh, H., Ogawa, Y., Tamura, N., Takaya, K., Igaki, T., Yamashita, J., Doi, K., Inoue, M., Masatsugu, K., Korenaga, R., Ando, J., Nakao, K. Shear stress augments expression of C-type natriuretic peptide and adrenomedullin. *Hypert.*, **1997**, *29*, 1296-1302.

[53] Garayoa, M., Martinez, A., Lee, S., Pio, R., An, W.G., Neckers, L., Trepel, J., Montuenga, L.M., Ryan, H., Johnson, R., Gassmann, M., Cuttitta, F. Hypoxia-inducible factor-1 (HIF-1) up-regulates adrenomedullin expression in human tumor cell lines during oxygen deprivation: a possible promotion mechanism of carcinogenesis. *Mol. Endocrinol.*, **2000**, *14*, 848-862.

[54] Champion, H.C., Akers, D.L., Santiago, J.A., Lambert. D.G., McNamara, D.B., Kadowitz PJ. Analysis of responses to human synthetic adrenomedullin and calcitonin gene-related peptides in the hindlimb vascular bed of the cat. *Mol. Cell Biochem.*, **1997**, *176*, 5-11.

[55] Shirai, M., Shimouchi, A., Ikeda, S., Ninomiya, I., Sunagawa, K., Kangawa, K., Matsuo, H. Vasodilator effects of adrenomedullin on small pulmonary arteries and veins in anaesthetized cats. *Br. J. Pharmacol.*, **1997**, *121*, 679-686.

[56] Eguchi, S., Hirata, Y., Kano, H., Sato, K., Watanabe, Y., Watanabe, T.X., Nakajima, K., Sakakibara, S., Marumo, F. Specific receptors for adrenomedullin in cultured rat vascular smooth muscle cells. *FEBS Lett.*, **1994**, *340*, 226-230.

[57] Ishizaka, Y., Ishizaka, Y., Tanaka, M., Kitamura, K., Kangawa, K., Minamino, N., Matsuo, H., Eto, T. Adrenomedullin stimulates cyclic AMP formation in rat vascular smooth muscle cells. *Biochem. Biophys. Res. Commun.*, **1994**, *200*, 642-646.

[58] Feng, C.J., Kang, B., Kaye, A.D., Kadowitz, P.J, Nossaman, B.D. L-NAME modulates responses to adrenomedullin in the hindquarters vascular bed of the rat. *Life. Sci.*,**1994**, *55*, L433-L438.

[59] Venema, R.C., Sayegh, H.S., Kent, J.D., Harrison, D.G.. Identification, characterization, and comparison of the calmodulin-binding domains of the endothelial and inducible nitric oxide synthases. *J. Biol. Chem.*, **1996**, *271*, 6435-6440.

[60] Nishimatsu, H., Suzuki, E., Nagata, D., Moriyama, N., Satonaka, H., Walsh, K., Sata, M., Kangawa, K., Matsuo, H., Goto, A., Kitamura, T., Hirata, Y. Adrenomedullin induces endothelium-dependent vasorelaxation *via* the phosphatidylinositol 3-kinase/Akt-dependent pathway in rat aorta. *Circ. Res.*, **2001**, *89*, 63-70.

[61] Owji, A.A., Smith, D.M., Coppock, H.A., Morgan, D.G., Bhogal, R., Ghatei, M.A., Bloom, S.R. An abundant and specific binding site for the novel vasodilator adrenomedullin in the rat. *Endocrinology,* **1995**, *136*, 2127-2134.

[62] Lippton, H., Chang, J.K., Hao, Q., Summer, W., Hyman, A.L. Adrenomedullin dilates the pulmonary vascular bed *in vivo*. *J. Appl. Physiol.*, **1994**, *76*, 2154-2156.

[63] Christman, B.W., McPherson, C.D., Newman, J.H., King, G.A., Bernard, G.R., Groves, B.M., Loyd, J.E. An imbalance between the excretion of thromboxane and prostacyclin metabolites in pulmonary hypertension. *N. Engl. J. Med.*, **1992**, *327*, 70-75.

[64] Tuder, R.M., Cool, C.D., Geraci, M.W., Wang, J., Abman ,S.H., Wright, L., Badesch, D., Voelkel, N.F. Prostacyclin synthase expression is decreased in lungs from patients with severe pulmonary hypertension. *Am. J. Respir. Crit. Care. Med.*, **1999**, *159*, 1925-1932.

[65] Giaid, A., Saleh, D. Reduced expression of endothelial nitric oxide synthase in the lungs of patients with pulmonary hypertension. *N. Engl. J. Med.*, **1995**, *333*, 214-221.

[66] Sata, M., Kakoki, M., Nagata, D., Nishimatsu, H., Suzuki, E., Aoyagi, T., Sugiura, S., Kojima, H., Nagano, T., Kangawa, K., Matsuo, H., Omata, M., Nagai, R., Hirata, Y. Adrenomedullin and nitric oxide inhibit human endothelial cell apoptosis *via* a cyclic GMP-independent mechanism. *Hypertension,* **2000**, *36*, 83-88.

[67] Kim, W., Moon, S.O., Sung, M.J., Kim, S.H., Lee, S., So, J.N., Park, S.K. Angiogenic role of adrenomedullin through activation of Akt, mitogen-activated protein kinase, and focal adhesion kinase in endothelial cells. *FASEB J.*, **2003**, *17*, 1937-1939.

[68] Pietra, G.G., Edwards, W.D., Kay, J.M., Rich, S., Kernis, J., Schloo, B., Ayres, S.M., Bergofsky, E.H., Brundage, B.H., Detre, K.M. Histopathology of primary pulmonary hypertension. A

qualitative and quantitative study of pulmonary blood vessels from 58 patients in the National Heart, Lung, and Blood Institute, Primary Pulmonary Hypertension Registry. *Circulation,***1989**, *80*, 1198-1206.

[69] Tuder, R.M., Groves, B., Badesch, D.B., Voelkel NF. Exuberant endothelial cell growth and elements of inflammation are present in plexiform lesions of pulmonary hypertension. *Am.J. Pathol.*, **1994**, *144*, 275-285.

[70] Kano, H., Kohno, M., Yasunari, K., Yokokawa, K., Horio, T., Ikeda, M., Minami, M., Hanehira, T., Takeda, T., Yoshikawa, J. Adrenomedullin as a novel antiproliferative factor of vascular smooth muscle cells. *J. Hypertens.*, **1996**, *14*, 209-213.

[71] Upton, P.D., Wharton, J., Coppock, H., Davie, N., Yang, X., Yacoub, M.H., Ghatei, M.A., Polak, J.M., Bloom, S.R., Smith, D.M., Morrell, N.W. Adrenomedullin expression and growth inhibitory effects in distinct pulmonary artery smooth muscle cell subpopulations. *Am. J. Respir .Cell. Mol. Biol.*, **2001**, *24*, 170-178.

[72] Horio, T., Kohno, M., Kano, H., Ikeda, M., Yasunari, K., Yokokawa, K., Minami, M., Takeda, T. Adrenomedullin as a novel antimigration factor of vascular smooth muscle cells. *Circ. Res.*, **1995**, *77*,660-664.

[73] Yoshihara, F., Nishikimi, T., Horio, T., Yutani, C., Takishita, S., Matsuo, H., Ohe, T., Kangawa, K. Chronic infusion of adrenomedullin reduces pulmonary hypertension and lessens right ventricular hypertrophy in rats administered monocrotaline. *Eur. J. Pharmacol.*, **1998**, *355*, 33-39.

[74] Chini, E.N., Chini, C.C., Bolliger, C., Jougasaki, M., Grande, J.P., Burnett, J.C., Jr, Dousa ,T.P. Cytoprotective effects of adrenomedullin in glomerular cell injury: central role of cAMP signaling pathway. *Kidney. Int.*, **1997**, *52*, 917-25.

[75] Matsui, H., Shimosawa, T., Itakura, K., Guanqun, X., Ando, K., Fujita, T. Adrenomedullin can protect against pulmonary vascular remodeling induced by hypoxia. *Circulation,***2004**, *109*, 2246-2251.

[76] Heaton, J., Lin, B., Chang, J.K., Steinberg, S., Hyman, A., Lippton, H. Pulmonary vasodilation to adrenomedullin: a novel peptide in humans. *Am .J. Physiol.*, **1995**, *268*, H2211-H2215.

[77] Yang, B.C., Lippton, H., Gumusel, B., Hyman, A., Mehta, J.L. Adrenomedullin dilates rat pulmonary artery rings during hypoxia: role of nitric oxide and vasodilator prostaglandins. *J .Cardiovasc. Pharmacol.*, **1996**, *28*, 458-462.

[78] Rademaker, M.T., Charles, C.J., Lewis, L.K., Yandle, T.G., Cooper, G.J., Coy, D.H., Richards, A.M., Nicholls, M.G. Beneficial hemodynamic and renal effects of adrenomedullin in an ovine model of heart failure. *Circulation,* **1997**, *96*, 1983-1990.

[79] Nagaya, N., Satoh, T., Nishikimi, T., Uematsu, M., Furuichi, S., Sakamaki, F., Oya, H., Kyotani, S., Nakanishi, N., Goto, Y., Masuda, Y., Miyatake, K., Kangawa, K. Hemodynamic, renal, and hormonal effects of adrenomedullin infusion in patients with congestive heart failure. *Circulation,* **2000**, *101*, 498-503.

[80] Nagaya, N., Nishikimi, T., Uematsu, M., Satoh, T., Oya, H., Kyotani, S., Sakamaki, F., Ueno, K., Nakanishi, N., Miyatake, K., Kangawa, K. Haemodynamic and hormonal effects of adrenomedullin in patients with pulmonary hypertension. *Heart,* **2000**, *84*, 653-658.

[81] Nishikimi, T., Horio, T., Yoshihara, F., Nagaya, N., Matsuo, H., Kangawa, K. Effect of adrenomedullin on cAMP and cGMP levels in rat cardiac myocytes and nonmyocytes. *Eur. J. Pharmacol.*, **1998**, *353*, 337-344.

[82] Ihara, T., Ikeda, U., Tate, Y., Ishibashi, S., Shimada, K. Positive inotropic effects of adrenomedullin on rat papillary muscle. *Eur. J. Pharmacol.*, **2000**, *390*, 167-172.

[83] Szokodi, I., Kinnunen, P., Tavi, P., Weckstrom, M., Toth, M., Ruskoaho, H. Evidence for cAMP-independent mechanisms mediating the effects of adrenomedullin, a new inotropic peptide. *Circulation,***1998**, *97*, 1062-1070.

[84] Hoeper, M.M., Schwarze, M., Ehlerding, S., Adler-Schuermeyer, A., Spiekerkoetter, E., Niedermeyer, J., Hamm, M., Fabel, H. Long-term treatment of primary pulmonary hypertension with aerosolized iloprost, a prostacyclin analogue. *N. Engl. J. Med.*, **2000**, *342*, 1866-1870.

[85] Walmrath, D., Schneider, T., Pilch, J., Grimminger, F., Seeger, W. Aerosolised prostacyclin in adult respiratory distress syndrome. *Lancet,* **1993**, *342*, 961-962.

[86] Nagaya, N., Okumura, H., Uematsu, M., Shimizu, W., Ono, F., Shirai, M., Mori, H., Miyatake, K., Kangawa, K. Repeated inhalation of adrenomedullin ameliorates pulmonary hypertension and survival in monocrotaline rats. *Am. J. Physiol. Heart. Circ. Physiol.*, **2003**, *285*, H2125-H2131.

[87] von der Hardt, K., Kandler, M.A., Chada, M., Cubra, A., Schoof, E., Amann, K., Rascher, W., Dotsch J. Brief adrenomedullin inhalation leads to sustained reduction of pulmonary artery pressure. *Eur. Respir. J.*, **2004**, *24*, 615-623.

[88] Yanagisawa, M., Kurihara, H., Kimura, S., Tomobe, Y., Kobayashi, M., Mitsui, Y., Yazaki, Y., Goto, K., Masaki, T. A novel potent vasoconstrictor peptide produced by vascular endothelial cells. *Nature,* **1988**, *332*, 411-415.

[89] Stewart, D.J., Levy, R.D., Cernacek, P., Langleben D. Increased plasma endothelin-1 in pulmonary hypertension: marker or mediator of disease? *Ann. Intern. Med.*, **1991**, *114*, 464-469.

[90] Nootens, M., Kaufmann, E., Rector, T., Toher, C., Judd, D., Francis, G.S., Rich, S. Neurohormonal activation in patients with right ventricular failure from pulmonary hypertension: relation to hemodynamic variables and endothelin levels. *J. Am. Coll. Cardiol.*, **1995**, *26*, 1581-1585.

[91] Rubens, C., Ewert, R., Halank, M., Wensel, R., Orzechowski, H.D., Schultheiss, H.P., Hoeffken G. Big endothelin-1 and endothelin-1 plasma levels are correlated with the severity of primary pulmonary hypertension. *Chest,* **2001**, *120*, 1562-1569.

[92] Collados, M.T., Velazquez, B., Borbolla, J.R., Sandoval, J., Masso, F., Montano, L.F., Guarner V. Endothelin-1 and functional tissue factor: a possible relationship with severity in primary pulmonary hypertension. *Heart Vessels,* **2003**, *18*, 12-17.

[93] Giaid, A., Yanagisawa, M., Langleben, D., Michel, R.P., Levy, R., Shennib, H., Kimura, S., Masaki, T., Duguid, W.P., Stewart, D.J. Expression of endothelin-1 in the lungs of patients with pulmonary hypertension. *N. Engl. J. Med.*, **1993**, *328*, 1732-1739.

[94] Nagaya, N., Kyotani, S., Uematsu, M., Ueno, K., Oya, H., Nakanishi, N., Shirai, M., Mori, H., Miyatake, K., Kangawa, K. Effects of adrenomedullin inhalation on hemodynamics and exercise capacity in patients with idiopathic pulmonary arterial hypertension. *Circulation,* **2004**, *109*, 351-356.

[95] Asahara, T., Murohara, T., Sullivan, A., Silver, M., van der Zee, R., Li, T., Witzenbichler, B., Schatteman, G., Isner JM. Isolation of putative progenitor endothelial cells for angiogenesis. *Science,* **1997**, *275*, 964-967.

[96] Takahashi, T., Kalka, C., Masuda, H., Chen, D., Silver, M., Kearney, M., Magner, M., Isner, J.M., Asahara, T. Ischemia- and cytokine-induced mobilization of bone marrow-derived endothelial progenitor cells for neovascularization. *Nat. Med.*, **1999**, *5*, 434-438.

[97] Gill, M., Dias, S., Hattori, K., Rivera, M.L., Hicklin, D., Witte, L., Girardi, L., Yurt, R., Himel, H., Rafii, S. Vascular trauma induces rapid but transient mobilization of VEGFR2(+)AC133(+) endothelial precursor cells. *Circ. Res.*, **2001**, *88*, 167-174.

[98] Kawamoto, A., Gwon, H.C., Iwaguro, H., Yamaguchi, J.I., Uchida, S., Masuda, H., Silver, M., Ma, H., Kearney, M., Isner, J.M., Asahara, T. Therapeutic potential of *ex vivo* expanded endothelial progenitor cells for myocardial ischemia. *Circulation,* **2001**, *103*, 634-637.

[99] Murohara, T., Ikeda, H., Duan, J., Shintani, S., Sasaki, K., Eguchi, H., Onitsuka, I., Matsui, K., Imaizumi, T. Transplanted cord blood-derived endothelial precursor cells augment postnatal neovascularization. *J .Clin. Invest.*, **2000**, *105*, 1527-1536.

[100] Shintani, S., Murohara, T., Ikeda, H., Ueno, T., Sasaki, K., Duan, J., Imaizumi, T.,Augmentation of postnatal neovascularization with autologous bone marrow transplantation. *Circulation,* **2001**, *103*, 897-903.

[101] Tateishi-Yuyama. E., Matsubara, H., Murohara. T., Ikeda, U., Shintani, S., Masaki, H., Amano, K., Kishimoto, Y., Yoshimoto, K., Akashi, H., Shimada, K., Iwasaka, T., Imaizumi, T. Therapeutic Angiogenesis using Cell Transplantation (TACT) Study Investigators. Therapeutic angiogenesis for patients with limb ischaemia by autologous transplantation of bone-marrow cells: a pilot study and a randomised controlled trial. *Lancet,* **2002**, *360*, 427-435.

[102] Nagaya, N., Kangawa, K., Kanda, M., Uematsu, M., Horio, T., Fukuyama, N., Hino. J., Harada-Shiba, M., Okumura, H., Tabata, Y., Mochizuki, N., Chiba, Y., Nishioka, K., Miyatake., K., Asahara, T., Hara, H., Mori, H. Hybrid cell-gene therapy for

pulmonary hypertension based on phagocytosing action of endothelial progenitor cells. *Circulation,* **2003,** *108,* 889-895.

[103] Murasawa, S., Llevadot, J., Silver, M., Isner, J.M., Losordo, D.W., Asahara, T. Constitutive human telomerase reverse transcriptase expression enhances regenerative properties of endothelial progenitor cells. *Circulation,* **2002,** *106,* 1133-1139.

[104] Fukunaka, Y., Iwanaga, K., Morimoto, K., Kakemi, M., Tabata, Y. Controlled release of plasmid DNA from cationized gelatin hydrogels based on hydrogel degradation. *J. Control. Release,* **2002,** *80,* 333-343.

[105] Kushibiki, T., Tomoshige, R., Fukunaka, Y., Kakemi, M., Tabata, Y. *In vivo* release and gene expression of plasmid DNA by hydrogels of gelatin with different cationization extents. *J. Cont. Release,* **2003,** *90,* 207-216.

[106] Kasahara, H., Tanaka, E., Fukuyama, N., Sato, E., Sakamoto, H., Tabata, Y., Ando, K., Iseki, H., Shinozaki, Y., Kimura, K., Kuwabara, E., Koide, S., Nakazawa, H., Mori, H. Biodegradable gelatin hydrogel potentiates the angiogenic effect of fibroblast growth factor 4 plasmid in rabbit hindlimb ischemia. *J. Am. Coll. Cardiol.,* **2003,** *41,* 1056-1062.

[107] Tokunaga, N., Nagaya, N., Shirai, M., Tanaka, E., Ishibashi-Ueda, H., Harada-Shiba, M., Kanda, M., Ito, T., Shimizu, W., Tabata, Y., Uematsu, M., Nishigami, K., Sano, S., Kangawa, K., Mori ,H. Adrenomedullin gene transfer induces therapeutic angiogenesis in a rabbit model of chronic hind limb ischemia: benefits of a novel nonviral vector, gelatin. *Circulation,* **2004,** *109,* 526-531.

Received: 18 April, 2005 Revised: 17 January, 2006 Accepted: 16 February, 2006

0013-7227/06/$15.00/0
Printed in U.S.A.

Endocrinology 147(4):1642–1653

doi: 10.1210/en.2005-1038

The Neuroprotective and Vasculo-Neuro-Regenerative Roles of Adrenomedullin in Ischemic Brain and Its Therapeutic Potential

Kazutoshi Miyashita, Hiroshi Itoh, Hiroshi Arai, Takayasu Suganami, Naoki Sawada, Yasutomo Fukunaga, Masakatsu Sone, Kenichi Yamahara, Takami Yurugi-Kobayashi, Kwijun Park, Naofumi Oyamada, Naoya Sawada, Daisuke Taura, Hirokazu Tsujimoto, Ting-Hsing Chao, Naohisa Tamura, Masashi Mukoyama, and Kazuwa Nakao

Department of Medicine and Clinical Science (K.M., H.I., H.A., N.S., Y.F., M.S., K.Y., T.Y.-K., K.P., N.O., N.S., D.T., H.T., N.T., M.M., K.N.), Kyoto University Graduate School of Medicine, Kyoto 606-8507, Japan; Department of Molecular Medicine and Metabolism (T.S.), Medical Research Institute, Tokyo Medical and Dental University, Tokyo 101-0062, Japan; and Department of Medicine (T.-H.C.), National Cheng-Kung University Medical Center, Tainan, Taiwan 701, Republic of China

Adrenomedullin (AM) is a vasodilating hormone secreted mainly from vascular wall, and its expression is markedly enhanced after stroke. We have revealed that AM promotes not only vasodilation but also vascular regeneration. In this study, we focused on the roles of AM in the ischemic brain and examined its therapeutic potential. We developed novel AM-transgenic (AM-Tg) mice that overproduce AM in the liver and performed middle cerebral artery occlusion for 20 min (20m-MCAO) to examine the effects of AM on degenerative or regenerative processes in ischemic brain. The infarct area and gliosis after 20m-MCAO was reduced in AM-Tg mice in association with suppression of leukocyte infiltration, oxidative stress, and apoptosis in the ischemic core. In addition, vascular regeneration and subsequent neurogenesis were enhanced in AM-Tg mice, preceded by increase in mobilization of CD34$^+$ mononuclear cells, which can differentiate into endothelial cells. The vasculo-neuro-regenerative actions observed in AM-Tg mice in combination with neuroprotection resulted in improved recovery of motor function. Brain edema was also significantly reduced in AM-Tg mice via suppression of vascular permeability. *In vitro*, AM exerted direct antiapoptotic and neurogenic actions on neuronal cells. Exogenous administration of AM in mice after 20m-MCAO also reduced the infarct area, and promoted vascular regeneration and functional recovery. In summary, this study suggests the neuroprotective and vasculo-neuro-regenerative roles of AM and provides basis for a new strategy to rescue ischemic brain through its multiple hormonal actions. (*Endocrinology* 147: 1642–1653, 2006)

ADRENOMEDULLIN (AM) IS a potent vasodilating peptide comprising 52 amino acids, which was originally isolated from human pheochromocytoma tissues in 1993 as a substance to elevate cAMP concentration in platelets (1). It is secreted mainly from the vascular wall into circulating blood to reduce pre- and post-load on the heart via vasodilation, natriuresis, and suppression of aldosterone release. Intravenous administration of AM to patients with heart failure or pulmonary hypertension has already been initiated and beneficial hemodynamic effects have been reported (2).

First Published Online December 29, 2005

Abbreviations: AM, Adrenomedullin; ANCOVA, analysis of covariance; BP, blood pressure; BrdU, bromodeoxyuridine; CGRP, calcitonin gene-related peptide; diHE, dihydroethidium; GFAP, glial fibrillary acidic protein; LDPI, laser Doppler perfusion imager; MCA, middle cerebral artery; 20m-MCAO, middle cerebral artery occlusion for 20 min; NeuN, neuronal marker; NHNP, normal human neuronal progenitor cells; PAMP, proadrenomedullin N-terminal 20 peptide; PECAM, platelet endothelial cell adhesion molecule; PI3K, phosphatidyl inositol-3 kinase; PKA, protein kinase A; ROS, reactive oxygen species; ssDNA, single-strand DNA; Tg, transgenic; Wt, wild type.

Endocrinology is published monthly by The Endocrine Society (http://www.endo-society.org), the foremost professional society serving the endocrine community.

Along with its vasodilating effect, a number of studies have demonstrated various and significant effects of AM on the regulation of vascular structure, including its development, remodeling, and regeneration. Mice lacking the AM gene did not survive their embryonic stage and showed abnormal vasculature with sc hemorrhage (3, 4). Mice overexpressing AM in endothelial cells were revealed to be hypotensive and resistant to vascular remodeling such as neointima formation caused by cuff injury, and atherogenesis associated with a high-cholesterol diet (5). We have recently established that AM promotes endothelial regeneration in the wound healing assay using cultured endothelial cells and enhances neovascularization *in vivo* into sc implanted gel-plugs in mice (6, 7). We and others (8–11) have further demonstrated that the potentiating action of AM on vascular regeneration is mediated by activation of the phosphatidyl inositol-3 kinase (PI3K)-Akt pathway.

Recently, it has been known that AM is secreted from various organs including the heart, lung, kidney, adipose tissues, and central nervous system (12). Moreover, AM expression has been demonstrated to be markedly enhanced by ischemia through the activation of hypoxia-responsive elements in the AM gene via transcription factor hypoxia-inducible factor-1. In the central nervous system, where AM is

mainly expressed in neurons and the endothelium (13), it is reported that transient ischemia boosted AM expression for more than 15 d (14). However, the role of augmented AM has remained unclear for inconsistent previous results: three studies reported neuroprotective effects of AM by demonstrating reduction of infarct size after transient ischemia (15–17), whereas one study detected exacerbation of infarction as a result of AM infusion (14).

In this context, our study presented here focused on the roles of augmented AM in ischemic brain and examined its therapeutic potential. We generated new lines of transgenic mice that overproduce AM (AM-Tg) in the liver that mimics chronic AM administration. After inducing 20-min middle cerebral artery occlusion (20m-MCAO) to produce a nonfatal stroke model in the AM-Tg mice, we observed the long-term effects of AM on the ischemic brain up to postoperative d 56. We examined the mice for the recovery of blood flow in the ischemic region and impaired motor function after stroke, and immunohistochemically examined the ischemic striatum to determine effects of AM on neuronal loss/apoptosis, gliosis, leukocyte infiltration, oxidative stress, vascular regeneration, and neurogenesis after 20m-MCAO. In addition, another stroke model, 2-h middle cerebral artery occlusion (2 h-MCAO), was performed to observe the effect of AM in acute phase of the fatal stroke. *In vitro* studies using neuronal progenitor cells or rat pheochromocytoma PC12 cells were performed to examine direct antiapoptotic and neurogenic actions of AM on these neuronal cells. Finally, we investigated the effect of exogenous AM administration after 20m-MCAO to determine the appropriate amount and timing of AM treatment after cerebral ischemia.

Materials and Methods

Generation of transgenic mice which overproduce human AM but do not overproduce mature proadrenomedullin N-terminal 20 peptide (PAMP)

The AM gene contains coding regions for not only AM but also PAMP, a different vasodilating peptide. Amidation at their carboxyl terminals after their synthesis is needed for both AM and PAMP to exert their biological activity. The bioactive amidated forms are known as mature AM and mature PAMP, respectively. To identify the specific effects of AM, we generated a transgene construct with a point mutation on the PAMP amidation signal in the full-length AM gene cDNA. Guanine was substituted for cytosine on the 3′ end of the PAMP coding region so that glycine on the C′ terminal of the PAMP product was replaced with alanine. In this way, amidation and maturation of PAMP by peptidylglycine α-hydroxylase and α-hydroxyglycine N-C lyase were inhibited (Fig. 1A). The mutant AM gene cDNA was then inserted into a plasmid containing the human serum amyloid P component promoter, which is widely used to target gene expression specific to the liver. When the product is secreted from the liver, it mimics intravenous administration of the agent. The *Hin*dIII-*Xho*I fragment of the plasmid was microinjected into the pronucleus of fertilized C57BL/6J mice eggs.

The copy number of transgenes was quantified by means of genomic Southern blotting according to standard procedure. Plasma concentrations of human total AM and mature AM were measured with a commercially available immunoradiometric assay (Cosmic, Tokyo, Japan).

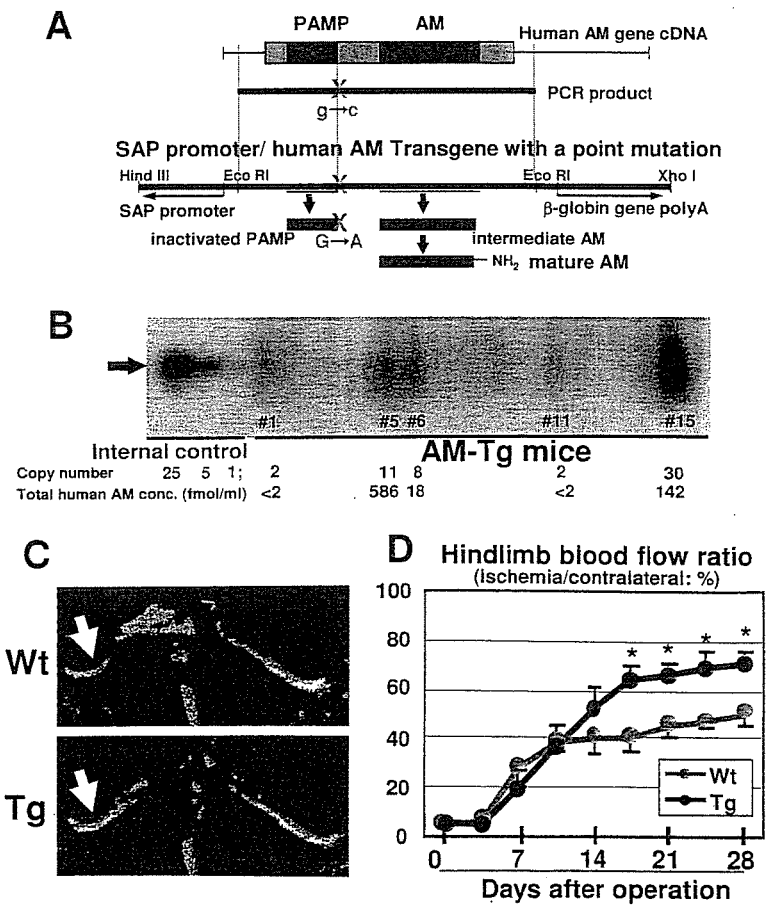

FIG. 1. Generation of transgenic mice which overproduce AM but do not overproduce mature PAMP in the liver and augmented angiogenesis in the transgenic mice after femoral artery occlusion. A, Schematic representation of the transgene construct derived from human AM gene cDNA with a point mutation in the amidation signal of PAMP. B, Southern blot analysis of the tail DNA of the founder mice. *Arrow*, Blots for the transgene. Internal controls for indicated copies are located in the *left three lanes*. The line No. indicates the mice in which the transgene was detected by PCR. The copy numbers estimated by densitometry and the plasma concentrations of total human AM in F3 mice of the lines are shown. C, Hindlimb blood flow analyzed by LDPI. *Red* or *white* indicates a higher flow than *blue* or *green*. *Arrows*, Comparison of ischemic hindlimbs between Wt and AM-Tg on d 28 after femoral artery ligation. D, Quantitative analysis of the hindlimb blood flow in ischemia. *, $P < 0.05$ for Wt *vs.* AM-Tg by ANCOVA; n = 6.

Human mature PAMP concentration was measured with a recently developed enzyme immunoassay (18). To determine the brain concentration of AM, we used the RIA kits for measurement of human and mouse total AM (Phoenix, Belmont, CA), according to the manufacturer's instruction. Blood pressure (BP) was measured with tail cuff (Softron, Tokyo, Japan). Hindlimb ischemia was induced by ligating the right femoral artery and blood flow of the ischemic limb was estimated with a laser Doppler perfusion imager (LDPI; Moor Instruments Ltd., Devon, UK) to confirm the angiogenic effect of AM-Tg mice. The perfusion ratio (%) was calculated as that of the ipsilatereal to the contralateral side. Animal care and experiments were in accordance with the guidelines for animal experiments of Kyoto University.

Induction of stroke by MCAO

We performed nonfatal 20m-MCAO and fatal 2 h-MCAO by the standard *trans*-luminal method, which has been described in various previous reports (19). Briefly, a 8–0 nylon monofilament coated with silicone was inserted from the left common carotid artery via the internal carotid to the base of the left middle cerebral artery (MCA) of 12-wk-old mice anesthetized with 5% halothane and maintained on 1%. After 20 min or 2 h of occlusion, the filament was withdrawn; and the arteries were reperfused, whereas the left common carotid artery was permanently ligated. Occlusion and reperfusion of the MCA was confirmed by means of fiber-shaped laser Doppler perfusion imager (Omegawave, Tokyo, Japan). We observed the mice until postoperative d 56 to examine blood flow in the ischemic region with an LDPI and motor function with a rota-rod exercise test.

Immunohistochemical examination of the ischemic striatum

After the induction of 20m-MCAO, mice were killed on postoperative d 0–56 and the harvested brains were subjected to immunohistochemical examination using a standard procedure described elsewhere (20). We used these primary antibodies: neuronal marker, NeuN (1:200; Chemi-Con, Temecula, CA); astrocyte marker, glial fibrillary acidic protein (GFAP) (1:400; Chemicon); apoptosis marker, single-strand DNA (ssDNA) (1:50; Dako, Carpinteria, CA); leukocyte marker, CD45 (1:100, PharMingen, San Diego, CA); endothelial marker, platelet endothelial cell adhesion molecule (PECAM)-1 (CD31) (1:100, PharMingen); and a marker for proliferating cells, bromodeoxyuridine (BrdU) (1:50, Molecular Probes, Eugene, OR); to examine infarct area, gliosis, leukocyte infiltration, apoptosis, vascular regeneration and neurogenesis. Briefly, free-floating 30-μm coronal sections at the level of the anterior commissure were stained and observed with a confocal microscope (LSM5 PASCAL; Carl Zeiss SMT AG, Oberkochen, Germany). The infarct area (mm^2/field) was defined and quantified as the region where loss of NeuN immunoreactivity was observed and gliosis (mm^2/field) as the area stained GFAP in the ischemic striatum at × 5 fields. CD45 or ssDNA-positive cells (cells/mm^2) were quantified to serve as an index of leukocyte infiltration or of apoptosis, respectively, in the ischemic core at ×20 magnification. Capillary density was quantified as the number of PECAM-1-positive cells (cells/mm^2). The vessel counts were performed in the region of ischemic core at 0.5~1.0 mm anterior from the bregma. We prepared two thin sections (6 μm thickness) per mouse for vessel counting and four representative fields from each section were evaluated for capillary density in the ischemic core. To examine neurogenesis, mice were injected ip with BrdU 50 mg/kg (Sigma-Aldrich Co., St. Louis, MO) twice daily on postoperative d 4–6 and the number of BrdU-NeuN double-positive cells (cells/mm^2), which are generally defined as regenerated neurons, were quantified to serve as an index of neurogenesis. We also examined the production of reactive oxygen species (ROS) *in situ* by using the oxidative fluorescent dye dihydroethidium (diHE; 2×10^{-6} M; Sigma).

Quantification of CD34$^+$ mononuclear cells after 20m-MCAO

We counted peripheral $CD34^+$ mononuclear cells according to the International Society of Hematotherapy and Graft Engineering (ISHAGE) guidelines (21). Briefly, peripheral blood was taken from the orbital vein and stained with CD34-PE and CD45-FITC monoclonal antibodies (BD PharMingen, San Jose, CA) in a TruCOUNT tube (BD PharMingen) according to the manufacturer's instruction. After the reaction, $CD34^+$-$CD45^{dim}$ cells were quantified as $CD34^+$ mononuclear cells by a fluorescence-activated cell sorting machine Aria (BD) by using the ISHAGE sequential gating strategy (21).

Analysis of infarct volume and brain edema after 2 h-MCAO

We performed 2 h-MCAO to examine the effect of AM in the acute phase of fatal stroke. To estimate infarct or edema volume, mice were killed 24 h after the occlusion. The brain was removed and cut into 2 mm-thick slices and immersed in saline containing 2% 2,3,5-triphenyltetrazolium chloride for 30 min at 4 C. Infarct or edema volume was calculated as the percentage volume of the contralateral hemisphere with a standard procedure as described elsewhere (22). We estimated Evans Blue leakage in the brain parenchyma as previously reported (23), to serve as an index of vascular permeability *in situ*. Briefly, 0.2 ml of 2.5% Evans Blue solution was injected into mice via a tail vein 10 min before 2 h-MCAO and mice were killed at 24 h after the ischemia. Brain tissues were weighed and homogenized in 50% trichloroacetic acid solution to extract the dye in the supernatant. The tissue content of Evans Blue was estimated from the absorbance of 620 nM.

Estimation of apoptosis and differentiation of neuronal cells

The ratio of apoptotic cells was examined using normal human neuronal progenitor cells (NHNP; Cambrex Bioscience, Walkersville, MD). Cells were plated at a density of 5×10^4 cells/cm^2 on a laminin-coated 24-well dish and incubated in serum-free neuronal basal medium for 48 h. After the experimental period, the cell number was assessed by 5-mercapto-1-methyltetrazole assay (Nakalai Tesque), and the cells were stained with an anti-ssDNA antibody and nuclear staining propidium iodide to calculate the ratio of apoptotic cells to the total cells in each microscopic image.

Neuronal differentiation was examined as described previously (24), using rat pheochromocytoma PC12 cells (Riken Gene Bank, Tsukuba, Japan). Briefly, the length of the neuronal process (micrometers/cell) was calculated to serve as an index of neuronal differentiation after plating at a density of 10^4 cells/cm^2 on a collagen I-coated 24-well dish and incubated in 1% serum DMEM for 7 d. The cells were treated with 10^{-5}mol/liter AM or 100 ng/ml nerve growth factor as a positive control, and with the following inhibitors: the two AM antagonists, 10^{-5}mol/liter AM (22–52) and 10^{-5} mol/liter calcitonin gene-related peptide(8–37) [CGRP(8–37)] (Peptide Institute Inc., Osaka, Japan), the two protein kinase A (PKA) inhibitors, 10^{-5} mol/liter adenosine 3P,5P-cyclic monophosphorothioate Rp-isomer (Rp-cAMP) and 10^{-6} mol/liter myristoylated cell-permeable PKA inhibitor peptide sequence (14–22) (PKA Inh), and the two PI3K inhibitors, 10^{-5} mol/liter LY294002 and 10^{-7} mol/liter wortmannin (Calbiochem, San Diego, CA). For endothelial cell coculture experiments, human umbilical vein endothelial cells (HUVEC; Cambrex) were plated into transwell membrane inserts at a density of 10^5 cells/cm^2.

Exogenous administration of AM and hydralazine

Recombinant human mature AM dissolved in 0.9% saline was exogenously administrated to C57BL/6J wild-type mice (Wt) by means of osmotic pumps (Alzet Model 2002; Alzet Osmotic Pumps Co., Cupertino, CA) at a rate of 50 ng/h, which is estimated to achieve a plasma concentration of 2 fmol/ml (25). To determine appropriate timing to start AM treatment after 20m-MCAO, we implanted the pump ip just after the operation (d 0), or at 24 (d 1) or 72 h (d 3) later. We killed the mice on d 7 for histological examination and the period of the exogenous AM treatment was from d 0, 1, or 3 to d 7. In some experiments, low-dose (0.1 mM) hydralazine was exogenously administrated in drinking water.

Statistics

All data were expressed as mean ± SE. Comparison of means between two groups was performed with Student's *t* test. When more than two groups were compared, ANOVA was used to evaluate significant differences among groups, and if significant differences were confirmed, each difference was further examined by means of multiple comparisons. We

TABLE 1. Plasma concentrations of human AM and systolic BP in Wt and three lines of AM-Tg mice

	Wt	Low conc.	Medium conc.	High conc.
Total AM (fmol/ml)	1.1 ± 0.2	17.6 ± 4.4[a]	142.2 ± 18.4[a]	585.5 ± 117.7[a]
Mature AM (fmol/ml)	0.5 ± 0.4	2.6 ± 0.6[a]	10.4 ± 2.4[a]	24.9 ± 4.2[a]
Systolic BP (mm Hg)	122.7 ± 1.6	113.0 ± 2.5[a]	113.4 ± 2.6[a]	109.4 ± 2.5[a]

conc., Concentration.
[a] $P < 0.01$ *vs.* Wt; n = 4–12.

performed analysis of covariance (ANCOVA) when repeated-measurement had done, specifically, in the rota-rod test and laser Doppler flowmetry. Probability was considered to be statistically significant at $P < 0.05$.

Results

Generation of transgenic mice that overproduce human AM but do not overproduce mature PAMP

We generated seven lines of founder mice carrying the transgene and maintained three of them (lines 5, 6, and 15). Their plasma concentrations of human total AM were 585.5 ± 117.7, 17.6 ± 4.4 and 142.2 ± 18.4 fmol/ml and the copy numbers of the transgene estimated by Southern blot densitometry analysis were 11, 8, and 30, respectively (Fig. 1B). The physiological concentration of mouse total AM is reportedly 5~10 fmol/ml, so that the transgenic mice were expected to overproduce AM about 100, 3, and 30 times more than endogenous AM. The three lines were designated low (no. 6), medium (no. 15), and high (no. 5) concentration line according to their plasma AM concentration. The high concentration line (no. 5) was used for further study unless otherwise indicated. The plasma concentration of human mature AM, the bioactive amidated form, increased to 2.6~24.9 fmol/ml in the AM-Tg mice (Table 1). On the other hand, plasma human mature PAMP did not change in AM-Tg mice. The concentration (fmol/ml) was 2.21 ± 0.58 in Wt *vs.* 2.15 ± 0.35 in AM-Tg (n = 6), so that the point mutation on the amidation signal in the PAMP coding region was expected to successfully inhibit maturation of PAMP. There were no apparent differences in overall appearance, behavior, growth or fertility between Wt and AM-Tg mice. The systolic BP in 12-wk-old mice was significantly reduced in all three lines of AM-Tg compared with Wt. The BP (mm Hg) was 122.7 ± 1.6 in Wt *vs.* 109.4 ± 2.5~113.4 ± 2.6 in AM-Tg, depending on the line ($P < 0.05$; n = 5; Table 1).

Therapeutic angiogenesis in hindlimb ischemia model was promoted in AM-Tg mice

The recovery of blood flow in the ischemic hindlimb of Wt and AM-Tg mice was compared and was found to have

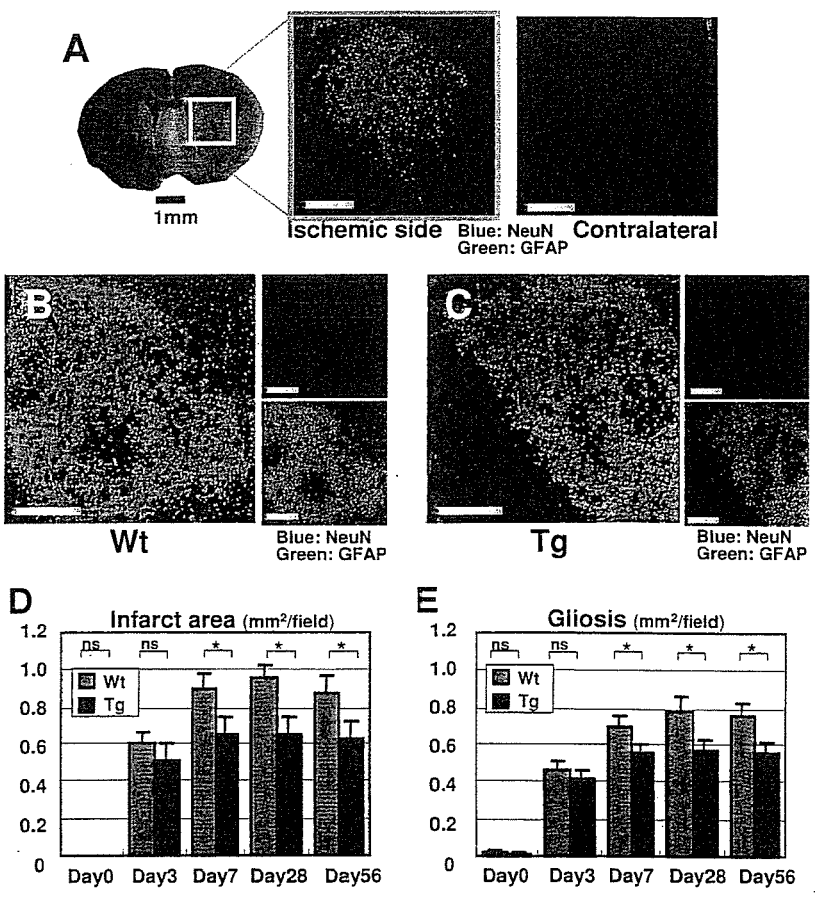

FIG. 2. Effects of AM on infarct area and gliosis after the nonfatal stroke, 20m-MCAO. A, Histological examination of the ischemic striatum. The outlined field was examined for infarct area and gliosis. The ischemic side and contralateral side on d 3 after 20m-MCAO are shown. *Scale bar*, 500 μm (×5 magnification). B and C, Representative images of the ischemic striatum on postoperative d 7 stained for NeuN (*blue*) and GFAP (*green*). Infarct area, defined as the region where NeuN immunoreactivity was lost, and gliosis, defined as the area where GFAP immunoreactivity was observed, in Wt (B) and AM-Tg (C) are shown. *Scale bar*, 500 μm (×5 magnification) D and E, Quantitative analysis of the infarct area (D) and gliosis (E) *, $P < 0.05$; ns, not significant for Wt *vs.* AM-Tg; n = 12.

significantly improved in AM-Tg mice after postoperative d 17. The hindlimb blood flow ratio on d 28 (ipsilateral/contralateral, %) was 56.6 ± 8.3 in Wt *vs.* 73.8 ± 5.3 in AM-Tg ($P < 0.05$; n = 6; Fig. 1, C and D). In this way, promotion of therapeutic angiogenesis by AM was confirmed in AM-Tg mice.

Brain remodeling in ischemic striatum after 20m-MCAO

We investigated the time course of neuronal loss, reactive gliosis, vascular regeneration, and neuronal regeneration; the entire process can be defined as "brain remodeling" after ischemia.

20m-MCAO caused selective loss of NeuN-positive cells and marked reactive gliosis (Fig. 2A) in the ipsilateral striatum within 24 h after the operation; this condition was different from pan-necrosis caused by longer MCAO (*e.g.* 2 h-MCAO). The infarct area, that is, the area of neuronal loss, expanded progressively up to d 7, and then showed gradual increase in size until d 56, whereas gliosis spread in parallel. The expansion of the infarct area in the subacute to chronic phase after mild stroke was compatible with previously reported findings (26). Vascular regeneration in the striatum with enhanced capillary density was obvious after postoperative d 7, and subsequent neurogenesis became obvious after d 28.

The concentrations of the overproduced human AM (fmol/g tissue) in the ischemic brain of AM-Tg mice before and on postoperative d 1 and 28 after 20m-MCAO were 27.8 ± 10.3, 87.4 ± 4.0 and 30.3 ± 16.8, respectively. Those of endogenous mouse AM (fmol/g tissue) were 3.7 ± 2.1, 7.2 ± 2.5, and 4.6 ± 3.0.

Infarct area and gliosis were reduced in AM-Tg mice after 20m-MCAO along with suppression of leukocyte infiltration and ROS production

A significant decrease in infarct area and gliosis was observed in AM-Tg mice (Fig. 2, B–E) after postoperative d 7, but was not obvious on d 3. The infarct area (mm^2/field) on d 56 was 0.88 ± 0.08 in Wt *vs.* 0.64 ± 0.08 in AM-Tg ($P < 0.05$; n = 12; Fig. 2D), and gliosis (mm^2/field) on the same day was 0.76 ± 0.08 in Wt and 0.56 ± 0.07 in AM-Tg ($P < 0.05$; n = 12; Fig. 2E). Leukocyte infiltration quantified as the number of $CD45^+$ cells was significantly suppressed in AM-Tg mice especially from d 3–7. $CD45^+$ cells on d 3 (/mm^2) numbered 197.5 ± 16.6 in Wt *vs.* 140.7 ± 14.6 in AM-Tg ($P < 0.05$; n = 12; Fig. 3, A, B, and G). *In situ* ROS production detected by immunostaining for diHE, which stained the nucleus of $NeuN^+$ or $GFAP^+$ cells, was enhanced in Wt compared with that in AM-Tg mice (Fig. 3, C and D). Apoptotic cells quantified as the number of $ssDNA^+$ cells in the ischemic core were significantly reduced in the AM-Tg mice on d 3–7. $ssDNA^+$ cells (/mm^2) on d 3 numbered 214.8 ± 19.6 in Wt *vs.* 123.2 ± 11.1 in AM-Tg ($P < 0.01$; n = 12; Fig. 3, E, F, and H).

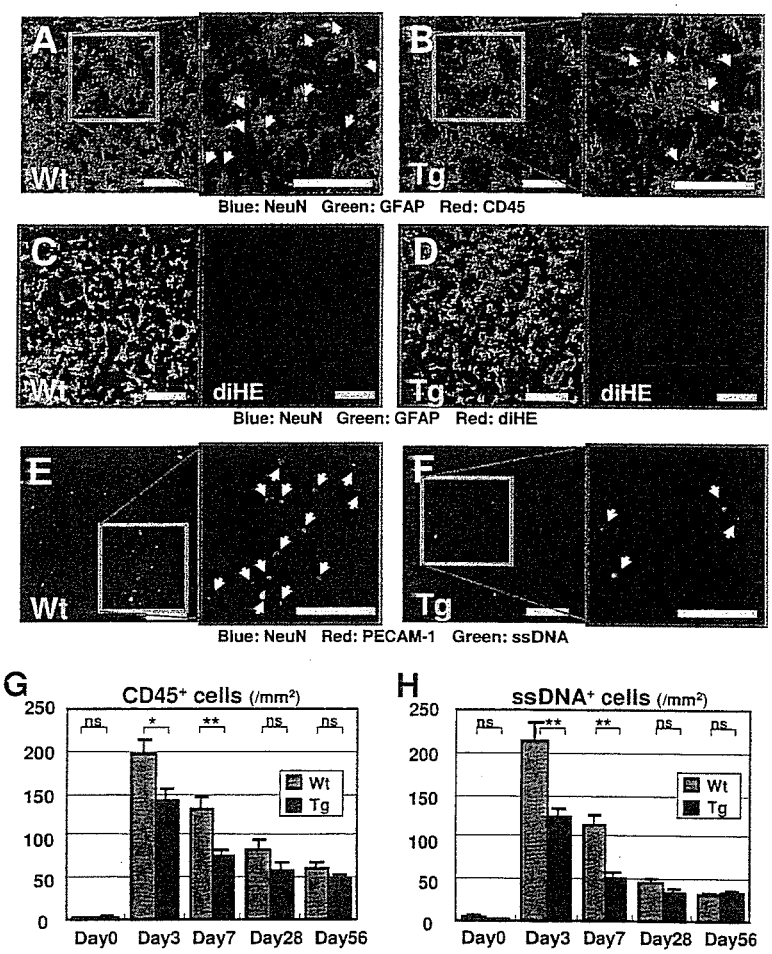

FIG. 3. Effects of AM on leukocyte infiltration, ROS production, and apoptosis in the ischemic brain after 20m-MCAO. A and B, Detection of leukocyte infiltration in the ischemic core on postoperative d 7 by immunostaining for $CD45^+$ cells (*red*) in Wt (A) and AM-Tg (B). *Arrows*, $CD45^+$ cells. C and D, *In situ* detection of ROS in ischemic striatum on postoperative d 7 by immunostaining for diHE (*red*) in Wt (C) and AM-Tg (D). E and F, Detection of apoptotic cells in the ischemic core on postoperative d 7 by immunostaining for $ssDNA^+$ cells (*green*) in Wt (E) and AM-Tg (F). *Arrows*, $ssDNA^+$ cells. G and H, Quantitative analysis of $CD45^+$ cells (G) and $ssDNA^+$ cells (H) in the ischemic core. *, $P < 0.05$; **, $P < 0.01$; ns, not significant for Wt *vs.* AM-Tg; n = 12. *Scale bar*, 100 μm (×20 magnification).

Vascular regeneration was augmented in AM-Tg mice after 20m-MCAO associated with increased mobilization of CD34$^+$ mononuclear cells

The blood flow in the ischemic brain estimated by LDPI was significantly higher in AM-Tg mice after postoperative d 7 and higher flow was maintained until d 56. The brain blood flow ratio (ipsilateral/contralateral, %) on d 56 was 88.9 ± 2.8 in Wt *vs.* 97.6 ± 3.0 in AM-Tg ($P < 0.01$ by ANCOVA; n = 8; Fig. 4, C, D, and H). We were also able to confirm that capillary density determined as the number of PECAM-1$^+$ cells was augmented in AM-Tg mice. The density (/mm^2) on d 56 was 468.8 ± 21.8 in Wt *vs.* 536.6 ± 13.6 in AM-Tg ($P < 0.05$; n = 8; Fig. 4I). Thus, the physiological neovascularization in the ischemic core after stroke was augmented in AM-Tg mice. Peripheral CD34$^+$ mononuclear cells were physiologically enhanced after 20m-MCAO and further increased in AM-Tg mice on d 3–7. The cells (/ml) on d 3 numbered 1774 ± 272 in Wt *vs.* 3199 ± 562 in AM-Tg ($P < 0.05$; n = 6; Fig. 5, A–C).

Augmented neurogenesis and improved recovery of impaired neurological function were observed in AM-Tg mice after 20m-MCAO

BrdU injection on postoperative d 4~6 proved that most BrdU-positive cells were costained with GFAP (data not shown) and that there were far fewer BrdU-PECAM-1 or BrdU-NeuN double-positive cells. We found that regenerated neurons defined as BrdU-NeuN double-positive cells were frequently detected adjacent to the vasculature and the number of these cells on d 56 was correlated with capillary density ($P = 0.003$; n = 12; Fig. 6, A and B; and Table 2). The cells increased from postoperative d 7–56, and their number was significantly higher in AM-Tg mice. The regenerated neurons (/mm^2) on d 56 numbered 20.4 ± 3.9 in Wt *vs.* 33.9 ± 4.7 in AM-Tg ($P < 0.05$; n = 12; Fig. 6C).

Recovery of impaired motor function after 20m-MCAO, quantified as the exercise time on an accelerating rota-rod from the start to collapse down, was significantly better in AM-Tg mice. The exercise time (second) on d 49 was 21.5 ± 1.5 for Wt *vs.* 27.1 ± 2.0 for AM-Tg ($P < 0.01$ by ANCOVA; n = 14; Fig. 6D). To confirm whether vasculogenesis and neurogenesis are the contributing factor to the recovery from the ischemic damage, we analyzed the relation between capillary density, the number of regenerated neuron and the rota-rod result in AM-Tg mice after 20m-MCAO. As shown in Table 2, we found that the capillary density was significantly correlated with the rota-rod exercise time ($P = 0.005$; n = 24) and neurogenesis tended to be correlated with it ($P = 0.08$; n = 12).

Low-concentration AM-Tg mice also showed reduced infarct area and promoted vascular regeneration

We performed 20m-MCAO, using the low-concentration AM-Tg mice (plasma mature AM, 2.6 ± 0.6 fmol/ml) as well as the high-concentration line (plasma mature AM, 24.9 ± 4.2 fmol/ml) to determine appropriate concentration for AM

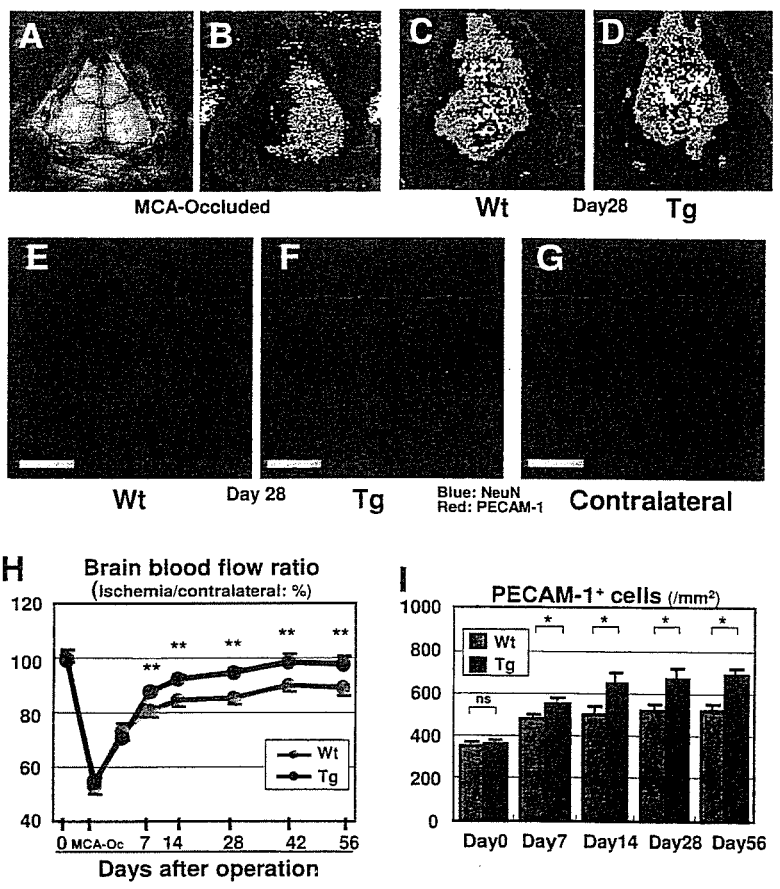

FIG. 4. Effects of AM on vascular regeneration in the ischemic brain after 20m-MCAO. A–D, Analysis of the blood flow in the ischemic brain by LDPI evaluated in mice with the scalp removed (A). Flowmetric analysis of the ischemic brain during MCA-Occlusion (B) and on d 28 after 20m-MCAO in Wt (C) and AM-Tg (D). *Red* or *white* indicates higher flow than *blue* or *green*. E–G, Histological examination of the vasculature in the ischemic core with PECAM-1 staining. Ischemic striatum on d 28 after 20m-MCAO in Wt (E) and AM-Tg (F), and contralateral nonischemic striatum (G). *Scale bar*, 100 μm (×20 magnification). H, Quantitative analysis of the blood flow in the ischemic brain. Comparison of recovery from ischemia after 20m-MCAO between Wt and AM-Tg. MCA-Oc, blood flow during MCA occlusion; **, $P < 0.01$ for Wt *vs.* AM-Tg by ANCOVA; n = 8. I, Quantitative analysis of capillary density in the ischemic brain. Comparison of time course for increase in capillary density, determined as the number of PECAM-1$^+$ cells, between Wt and AM-Tg mice. *, $P < 0.05$; ns, not significant; n = 8.